

Chemistry at Boron: Synthesis and Properties of Red to Near-IR Fluorescent Dyes Based on Boron-Substituted Diisoindolomethene Frameworks

Gilles Ulrich,^{*,†} Sébastien Goeb,^{†,§} Antoinette De Nicola,[†] Pascal Retailleau,[‡] and Raymond Ziessel^{*,†}

[†]Laboratoire de Chimie Moléculaire et Spectroscopies Avancées (LCOSA), ECPM, CNRS, 25 rue Becquerel, 67087 Strasbourg Cedex 02, France

[‡]Laboratoire de Crystallochimie, ICSN - CNRS, Bât 27 - 1 avenue de la Terrasse, 91198 Gif-sur-Yvette Cedex, France

[§]Laboratoire MOLTECH-Anjou, Groupe SOMaF, Université d'Angers, 2 bd Lavoisier, 49045 Angers Cedex, France

S Supporting Information

ABSTRACT: A general method for the synthesis of difluorobora-diisoindolomethene dyes with phenyl, *p*-anisole, or ethylthiophene substituents has been developed. The nature of the substituents allows modulation of the fluorescence from 650 to 780 nm. Replacement of the fluoro ligands by ethynyl-aryl or ethyl residues is facile using Grignard reagents. Several X-ray molecular structures have been determined, allowing establish-



R = F, Et, 4-tolylolethynyl or 1-pyrenylethynyl

ment of structure–fluorescence relationships. When the steric crowding around the boron center is severe, the aromatic substituents α to the diisoindolomethene nitrogens are twisted out of coplanarity, and hypsochromic shifts are observed in the absorption and emission spectra. This shift reached 91 nm with ethyl substituents compared to fluoro groups. When ethynyl linkers are used, the core remains flat, and a bathochromic shift is observed. All the fluorophores exhibit relatively high quantum yields for emitters in the 650–800 nm region. When perylene or pyrene residues are connected to the dyes, almost quantitative energy transfer from the dye core occurs, providing large virtual Stokes shifts spanning from 8000 to 13 000 cm^{-1} depending on the nature of the dye. All the dyes are redox active, providing the Bodipy radical cation and anion in a reversible manner. Stepwise reduction or oxidation to the dication and dianion is feasible at higher potentials. We contend that the present work paves the way for the development of a new generation of stable, functionalized luminophores for bioanalytical applications.

INTRODUCTION

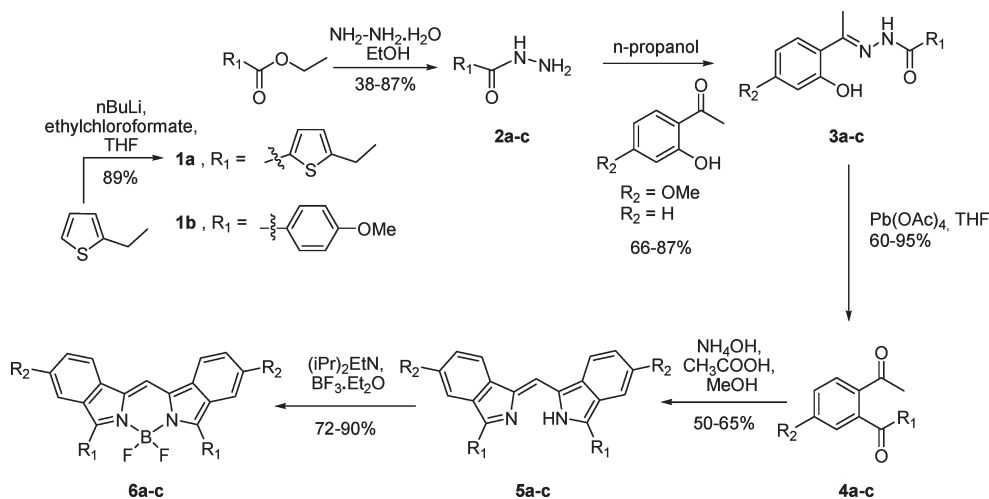
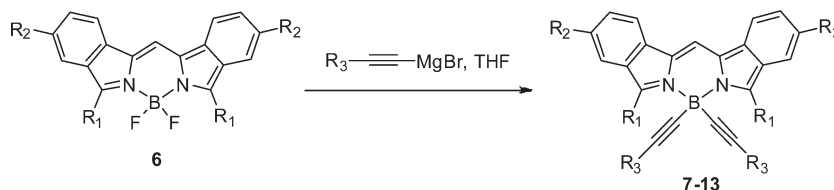
The existence of an absorption window of blood between 650 and 900 nm (due to concomitant low absorption and minimal autofluorescence of hemoglobin and water)¹ has stimulated research into the development of efficient fluorophores emitting in this particular spectral region. Such dyes should find numerous applications in noninvasive and *in vivo* fluorescence imaging² and mapping deeper tissues or DNA sequences.³ Before being used under biological conditions of analysis, they must, however, meet many criteria such as: (i) high absorption and high fluorescence quantum yields, (ii) solubility in various solvents without forming nonemissive aggregates, (iii) resistance to photodecomposition under intense light sources, (iv) pronounced Stokes shifts to facilitate signal detection, (v) low toxicity if *in vivo* analysis is intended. Existing red fluorophores from the cyanine family (e.g., CyDye, namely, Cy 5.0 and Cy 5) despite their high extinction coefficients suffer from low fluorescence quantum yields and limited photochemical stability. Nowadays most common red emitters are from the rhodamine family (Texas Red, Alexa...). They have good brightness, but they are essentially limited to the 650–700 nm region.⁴ There is an ongoing synthetic challenge for the development of brilliant red-NIR organic emitters which are soluble in

most common solvents including polar ones. Due to their special photophysical properties (high fluorescence quantum yields, large molar extinction coefficients, sharp fluorescence peaks) coupled to a chemical versatility and color tunability, the difluorobora-diaza-s-indacene family of Bodipy dyes represents a unique category of fluorophore.⁵ Several strategies have been used to bathochromically shift the emission of such dyes: (i) extension of the π conjugation of the cyanine core at the 3,5-^{6–9} or 2,6-positions,¹⁰ (ii) fusion of aromatic moieties onto the indacene skeleton,¹¹ (iii) replacement of the C8-carbon by a nitrogen, providing azaBodipy dyes,¹² (iv) decoration with electron-donating groups,¹³ and (v) fusion with a cyanine skeleton.¹⁴ However, most of these compounds suffer from the inherently low Stokes shifts characteristic of organic fluorophores, which is a major drawback in biological experiments, and there is a need to overcome this problem to enhance the sensitivity of the probes. Two strategies have been applied to excite the sample well away from the emission wavelength: (i) the use of two-photon excitation with suitable fluorophores¹⁵ or (ii) building a so-called cassette system by

Received: February 14, 2011

Published: April 18, 2011

Scheme 1. Synthesis of Diisoindolemethene Borates

Scheme 2. Synthesis of Homodisubstituted *E*-Bodipys

connection of an appropriate high-energy absorber to the emitting molecule.^{16,17} The latter was successfully applied to various Bodipys emitting in the green–orange region by attaching polyaromatic substituents to the Bodipy core¹⁸ or at the boron center.¹⁹ The cassette strategy was also recently successfully applied to a water-soluble Bodipy system used for monitoring interactions in living cells²⁰ and by attachment to Nile Red as an acceptor red-emitting dye.²¹

We present here our comprehensive investigations of cassette-like systems derived by the linking of diisoindolemethene-based Bodipys to polyaromatic chromophores.²² The chromophores have been connected to the boron atom via an ethynyl tether to prevent steric congestion inducing strong perturbation of the optical properties.²³

RESULTS AND DISCUSSION

A convenient sequence leading to the symmetrically substituted diisoindolemetheneboron difluoride compounds **6a–c** is depicted in Scheme 1.²⁴ It allows the nature of the substituents R_1 and R_2 on both sides to be changed through preparation of the precursor 2-acylacetophenones **4a–c**. These substituents have a direct influence on the resulting diazaboraindacene absorption and emission wavelengths.

Commercially available 2-acetylphenols bearing R_2 were reacted with benzo or thieno (R_1 group) carbohydrazides **2a–c**, obtained from their corresponding ethyl esters, to give acylhydrazones **3a–c**. The treatment of **3a–c** with lead tetraacetate led to intramolecular migration²⁵ and the replacement of the phenolic hydroxyl by the acyl substituent as in **4a–c**. The diisoindolemethenes **5a–c** were obtained by condensation of diketones

4a–c with an ammonium salt. In this reaction, the bis-isoindolymethane intermediate underwent formaldehyde elimination by a retro-aldol reaction before being oxidized by air.²⁶ Finally, the formation of **6a–c** was accomplished by reaction of **5a–c** with boron trifluoride in the presence of Hünig's base.

Developing upon our previous work performed on “cascadelle” dyes obtained by linking high-energy chromophores to the boron center of yellow Bodipy fluorophores via acetylenic bridges,^{18,27} we first attempted to connect similar polyaromatic fragments to a diisoindolemethene acceptor via the same procedure. The use of lithium acetylide was unsuccessful, leading to decomposition of the dye. We then decided to use a Grignard acetylide, known to be useful for substitution of halides on a trigonal boron center.²⁸ This choice was also based on the fact that reaction of a lithium alkyl with β -diketiminato boron(III) chelates results in attack at a ring carbon atom, whereas reaction with a Grignard results in substitution at boron.²⁹ A general procedure was optimized to synthesize the diisoindolemethene diacetylide (*E*-Bodipy)³⁰ derivatives (Scheme 2) by using a large excess (2.4–3 equiv) of the appropriate magnesium acetylide bromide, generated by addition of ethylmagnesium bromide to an anhydrous THF solution of the arylacetylene. This solution was heated at 60 °C prior to use, to ensure complete formation of the Grignard. The acetylide was then added to diisoindolemethene difluoride derivatives **6a–c** at room temperature, and the mixture was heated overnight at 60 °C. Standard workup and chromatography on silica afforded the desired compounds, and the average yields are given in Table 1. Several compounds obtained by varying the high-energy donor as well as the low-energy emitters were prepared with satisfactory yields, which were not dependent on the nature and size of the polyaromatic substituents R_3 . No monoacetylide derivatives were detected,

Table 1. Summary of the Different Substituents of the Homodisubstituted Diisoindolomethene Borates

Entry	R ₁	R ₂	R ₃	Isolated Yields (%)	¹¹ B NMR ^a
7		OMe		46	-6.3
8		OMe		62	-7.3
9		OMe		29	-6.4
10		OMe		76	-7.4
11		OMe		41	-6.7
12		OMe		49	-6.9
13		H		42	-7.1

^a Calibrated referring to residual glass B₂O₃.

but small amounts (<5%) of starting material did remain. It seems that the formation of the first B–Csp bond favors the attack of a second molecule of magnesium bromide acetylide on the boron. The fluoride substitution is easily monitored by ¹¹B NMR, where disappearance of the characteristic triplet of B bound to two fluorines is observed and a highly shielded singlet appears (Table 1).

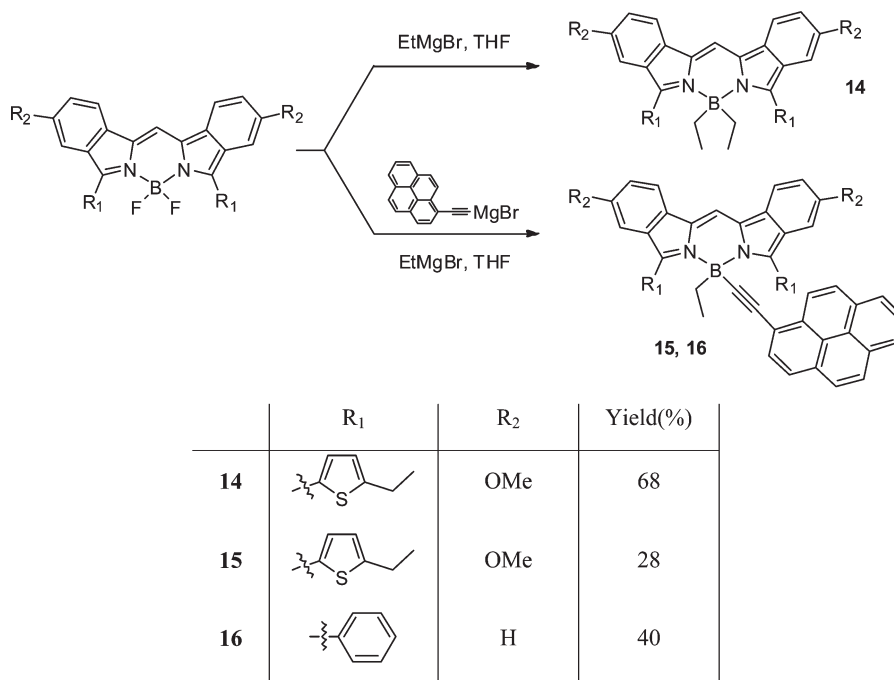
Fortuitously, the conditions under which the alkyl-substituted compound **14** was obtained provided the key for the synthesis of the boron heterodisubstituted derivatives **15** and **16** (Scheme 3). The reaction of ethylmagnesium bromide with **6a** at RT appeared to be almost instantaneous, and the diethylboron compound **14** was obtained in 68% yield after purification. Taking this to mean that the intermediate monoethyl compound must be highly activated toward all nucleophiles, the reaction was conducted using an equimolar mixture of ethyl- and ethynyl-magnesium bromides and, gratifyingly, was found to lead to a mixture of diethyl-, dialkynyl-, and alkynylethylboron derivatives which could be easily separated by flash chromatography (Scheme 3).

This procedure provided a means to introduce two different molecular subunits on the boron center, one carrying a polyaromatic residue and the second a masked function. One of our objectives here was to introduce an pyrenylethynyl unit as well as a substituent which could function as a potential anchoring arm (an activated succinic-ester for instance see Scheme 5). The succinimidyl ester (NHS ester) group is an exceptionally useful grafting entity that, for example, preferentially acylates amino groups under mild reaction conditions. Thus, the coupling of biopolymers such as proteins can be envisaged. The first step in its synthesis was the preparation of the oxazoline **19**.

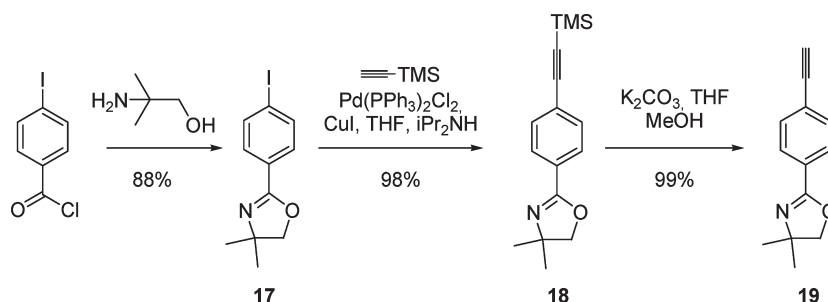
4-Iodobenzoylchloride was reacted with 2-amino-2-methylpropanol to give oxazoline **17**, which was subjected to Sonagashira coupling with trimethylsilylacetylene to give **18** in 98% yield. Deprotection of the acetylene unit using K₂CO₃ then provided **19** in essentially quantitative yield (Scheme 4).³¹ Dyes **20a–c** were obtained by the sequence of reactions listed in Scheme 5 where the reaction of derivatives **6a–c** with a mixture of the Grignards from compound **19** and from ethynylpyrene gave **20a** 43%, **20b** 56%, and **20c** 9%. Various reaction conditions were explored to transform the oxazoline function into carboxylic ester without degradation of the dibenzopyrromethene backbone and substitution on the boron center. Hydrolysis in a mixture of aqueous 3 M H₂SO₄ and THF proved effective for compounds **20a–c**. The resulting polar amino-esters were transesterified to facilitate purification. Thus, reaction with sodium methoxide gave the methyl esters in good yields (**21a** 80%, **21b** 67%, **21c** 86%). To assess its suitability for biolabeling, compound **21a** was hydrolyzed with NaOH at room temperature overnight. The crude acid obtained by neutralizing the product solution with NH₄Cl was treated at room temperature with *N*-hydroxysuccinimide in the presence of 1-[3-(dimethylamino)propyl]-3-ethylcarbodiimide (EDCI) and 4-dimethylaminopyridine (DMAP) to give the activated ester in good yield (67%), and as expected, reaction of *n*-propylamine with this NHS ester led instantaneously to the amide **22a** (81%).

X-ray Structure Determinations. Single-crystal X-ray diffraction measurements provided the molecular structures of compounds **6c**, **8**, **11**, **13**, **14**, **15**, and **16**, confirming the identity expected on the basis of their synthesis and defining, in particular,

Scheme 3. Approaches to Heterodisubstituted Diisoindolemethene Borates



Scheme 4. Synthesis of 4-Ethynyl-1-(dimethyloxazolidinyl)-benzene



the influence of the boron substituents on the planarity of the edifice (Figures 1–7). Characteristic bond lengths and angles are reported in Table 2. In all structures, the boron atom has a distorted tetrahedral environment. N–B–N angles fall within the range for known species [mean $106.34(12)^\circ$ from 200 hits found in the Cambridge Structural Database (CSD version 5.31, with August 2010 updates)],³² but the C–B–C angle is slightly larger than that observed in *C*- or *E*-borondipyromethenes³⁰ [$115.2(5)^\circ$ from 16 hits]. The average B–N bond length is slightly longer than that for the corresponding *F*-Bodipy.³³ The average N1–C4/N2–C5 length is 1.36 Å, typical of this family of dyes, as is the longer bond length of 1.42 Å for N1–C1/N2–C8.³³ The elongated B–C bonds in **8** and **13–16** of ca. 1.59 Å are similar to those found in other *C*- or *E*-Bodipy. The triple bond character of the ethyne link is maintained, with an average bond length of 1.20 Å in **8**, **13**, **15**, and **16**. A slight distortion from planarity of the cyanine core is observed as previously described for Bodipys bearing bulky groups in the 3,5-positions.³³ It may be described as a “butterfly” conformation, with the wings being the BN1C1C2C3C4C9 and BN2C5C6C7C8C9 planes. The dihedral angles are larger with phenyl substituents on the C4,

C5 ortho positions than with thiophene residues (ca. $9–12^\circ$ versus $2–6^\circ$).

A tilt between the R₁ aromatic groups located in the 3,5-positions and the indacene core is observed and may be indicative of the steric congestion induced by the boron substituent. The ethynyl substituents seem to minimize congestion around the boron center, and thus the tilt is very similar to that induced by fluorine (compare **6c** and **13**) (Figures 1 and 2). When the substituent is a flexible, saturated group such as ethyl, the tilt angle is much greater (**15** and **16**) (Figures 3 and 4), with the two bulky substituents (**14**) becoming almost orthogonal (Figure 5). Comparison of the thienyl-substituted compound structures shows that the sulfur atoms point in opposite directions in the homodisubstituted dyes **8** (Figure 6) and **14** but predominantly (in about 70% of molecules) in the ethynyl bond direction in the case of **15** (Figure 3). The crystal structure features of **11** (Figure 7) with two ethynylpyrene residues is similar to **13** bearing two ethynyltolyl fragments (Figure 2).

With respect to the molecular packing, each of the seven crystal structures displays inversion-related pairs of diisoindolemethene fragments with mean plane-to-plane distances ranging from 3.37 Å (**13**, Figure S1, Supporting Information) to 3.69 Å (**14**,

Scheme 5. Synthesis of Diisoindolemethene Borates Bearing Ethynylpyrene and Benzoic Acid Precursor Substituents on the Boron Center

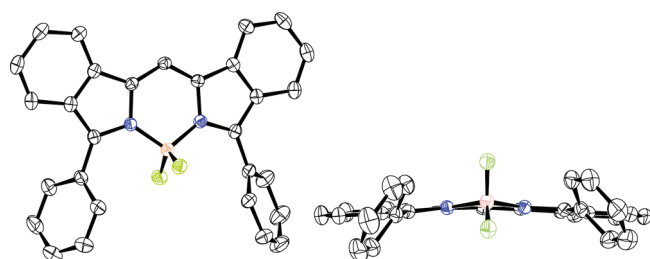
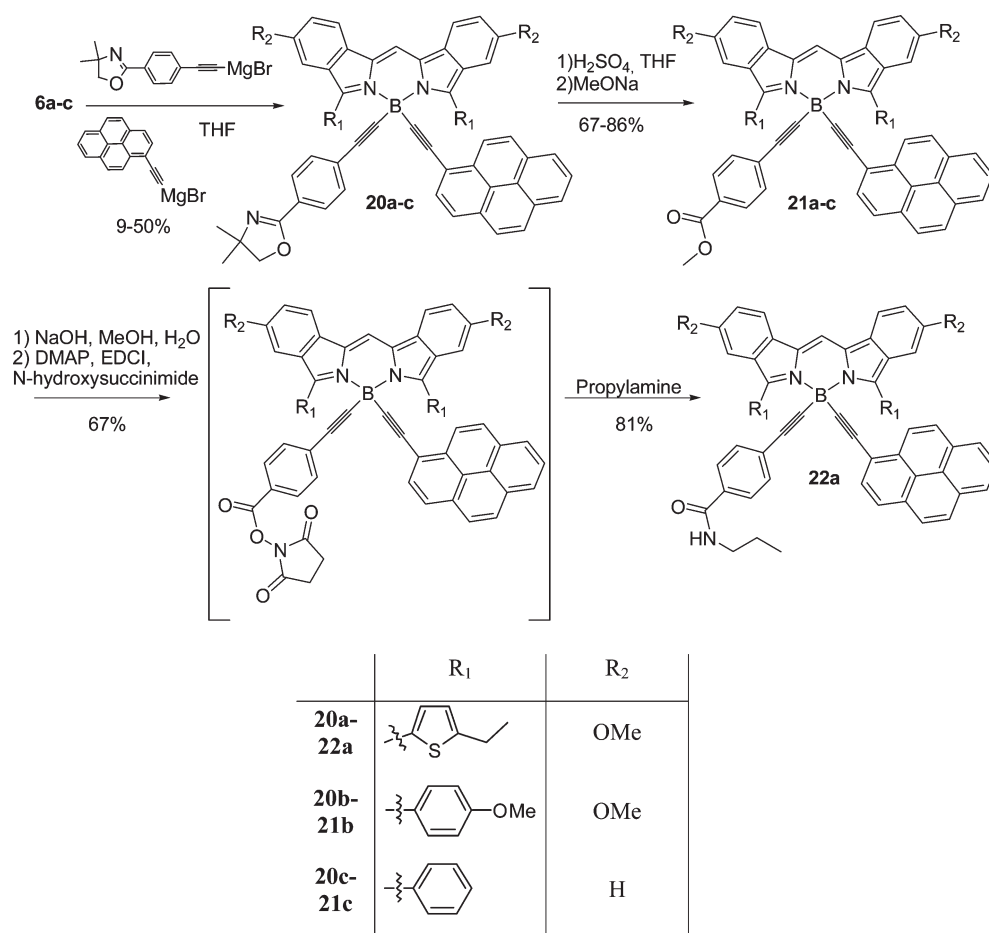


Figure 1. Orthogonal ORTEP views of the molecular structure of **6c**. (Here and in all other figures, probability displacement ellipsoids are shown at the 30% level.)

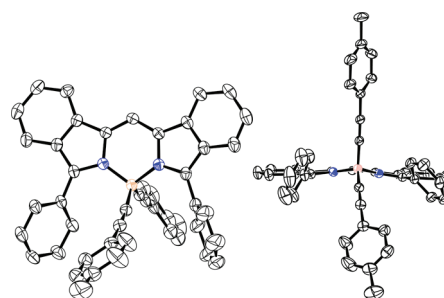


Figure 2. Orthogonal ORTEP views of the molecular structure of **13**.

Figure S2, Supporting Information). The absence of cumbersome substituents at the boron atom for **6c** results in the formation of infinite stacks of **6c** molecules along the *a* direction. In the case of **14**, the greatest overlap is found between the outer phenyl groups with a centroid–centroid distance of 3.655(2) Å (Figure S2, Supporting Information). Pyrene interactions with an interplanar distance of 3.431 Å, parallel to (100), and sandwiched here by edge-to-face interactions with the outer phenyl groups of pairs of diisoindolemethene groups are observed for compound **16** (Figure 8). Similar packing is seen in compounds **11** (Figure 9) and **15** (Figure S3,

Supporting Information) with 3.428 and 3.483 Å pyrene-to-pyrene distances and with methoxy groups or thiophene groups, respectively, on both sides of the pairs of pyrenes.

Electrochemical Properties. Cyclic voltammetry in dichloromethane solution was used to probe the electronic effects of the various substituents on the Bodipy electrophore. Table 3 lists the potentials (relative to the SCE reference electrode) for the waves observed in the +1.6 to –2.2 V windows.

For the starting materials **6a**, **6b**, and **6c**, a single anodic wave, safely assigned to the (Bodipy/Bodipy⁺) couple, was observed in the region between +0.73 and +0.43 V (Figure 10). All were reversible ($i_{pa}/i_{pc} \approx 1$), with a shape characteristic of a Nernstian

Table 2. Selected Geometric Parameters Deduced from the X-ray Structural Data

comps	average B–N (Å)	average B–X (Å)	average C4/ 5=N (Å)	average C4/ 5–C3/6 (Å)	N1–B–N2 (deg)	X1–B–X2 (deg)	dihedral angles diisindolomethene/R1	dihedral angles BN1C1C2C3C4C9/ BN2C5C6C7C8C9
6c	1.57	1.38	1.35	1.42	107.9 (1)	110.9(1)	59.2/54.4 58.8/54.1	8.6 8.7
8	1.60	1.58	1.36	1.43	107.4 (3)	118.1(3)	54.4/32.3	1.7
11	1.59	1.58	1.36	1.43	107.2 ± 0.3	116.9 ± 0.7	68.1/38.1 84.5/65.4–45.2	9.2 ± 2.2
13	1.59	1.58	1.35	1.42	106.6 (1)	118.4(1)	68.2/53.4 67.5/53.2	12.3
14	1.61	1.61	1.35	1.42	105.0(2)	115.1(2)	81.1/78.8	6.0
15	1.60	1.59	1.36	1.43	106.4 (3)	112.7(3)	61.1/ 83.9–65.0	4.9
16	1.59	1.58	1.35	1.39	106.6(3)	117.8(3)	69.9/65.3 68.6/65.6	9.0

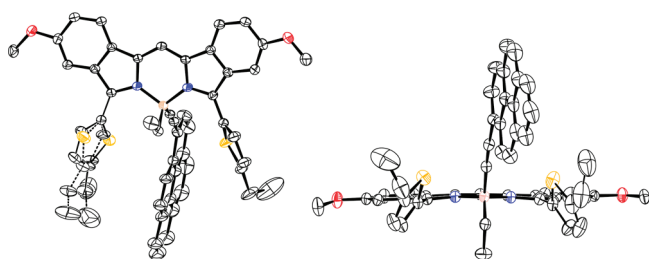


Figure 3. Orthogonal ORTEP views of the molecular structure of 15.

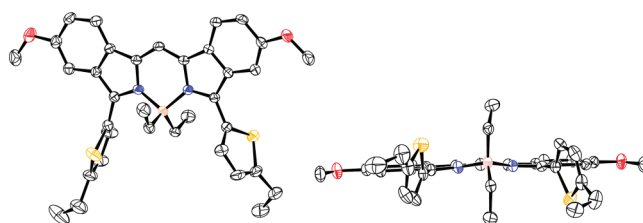


Figure 5. Orthogonal ORTEP views of the molecular structure of 14.

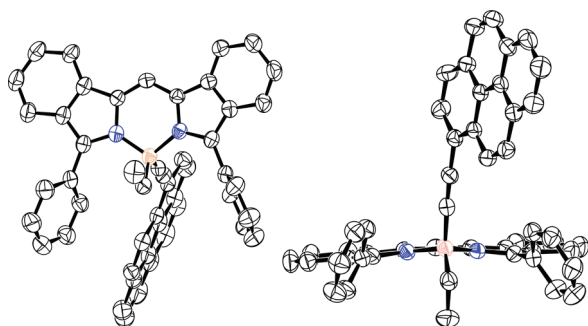


Figure 4. Orthogonal ORTEP views of the molecular structure of 16.

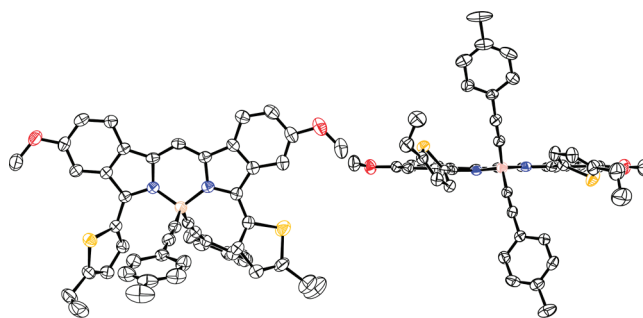


Figure 6. Orthogonal ORTEP views of the molecular structure of 8.

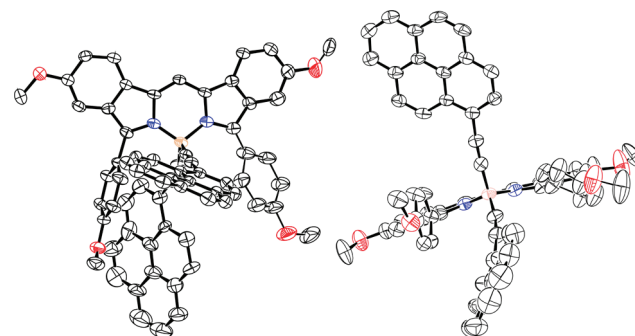


Figure 7. Orthogonal ORTEP views of the molecular structure of 11.

one-electron process ($\Delta E_p = 60\text{--}70$ mV). Note that this wave is less anodic for the dye substituted with ethylthiophene fragments (derived from **6a**) than for the anisole- and phenyl-substituted dyes (derived from **6b** and **6c**, respectively), the last being the most difficult to oxidize. This reflects the fact that the thiophene and anisole residues are better electron-donating groups than phenyl. Interestingly, oxidation of these blue and green dyes is easier by 370–670 mV relative to that of the yellow dyes of type A in Chart 1.³⁴

The second oxidation found at higher potential in the +1.3 to 1.59 V range for the same dyes is assigned to formation of the (Bodipy²⁺) dication and appears to be reversible for dyes **6a** and **6b** but irreversible for **6c**. The formation of Bodipy²⁺ dications has previously been observed in particular solvent conditions and when pyridine moieties are grafted onto the central position of the basic yellow molecules.³⁴

Dyes **6a**, **6b**, and **6c** are also reducible, displaying a reversible reduction to the radical anion (Bodipy^{•-}) in the range -0.92 to -1.08 V and an irreversible reduction to the dianion (Bodipy²⁻) at more cathodic potentials (Table 3). It is interesting to note

that the HOMO–LUMO gaps of 1.35 eV for **6a**, 1.58 eV for **6b**, and 1.79 eV for **6c** are in keeping with the bathochromic shift of the emission wavelength for the corresponding dyes in dilute solution (*vide infra*).

Surprisingly, along a series of dyes constructed from the same skeleton, for instance, the ethylthienyl derivative of **6a**, the substitution of both fluoro groups with an arylethynyl or alkyl fragment has little effect on the first oxidation potential, which remains around +0.41 V. This is in strong contrast with the previous observation made for the yellow dyes **A** and **B**, where fluoride substitution leading to dyes **C** resulted in a shift of ~100 mV toward the anodic region for both the radical cation and radical anion, although the HOMO/LUMO gap remained similar to that of molecules **A** and **B**.^{18b,22} However, note that the second oxidation process leading to the dication (Bodipy²⁺), with the exception of dye **14** where ethyl groups replace the fluoro residues, is difficult to compare due to the irreversibility of most of the processes. However, it seems that this second oxidation is facilitated and sensitive to the presence of the alkyne fragments on the boron center.

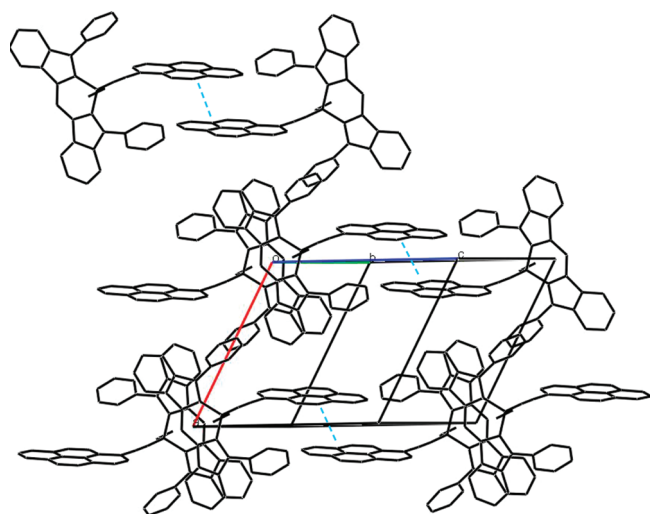


Figure 8. View of packing of compound **16** down the *b*–*c* direction. Cyan dashed lines indicate pyrene–pyrene stacking parallel to (100) between molecules at *x*, *y*, *z* and $-x$, $3 - y$, $1 - z$.

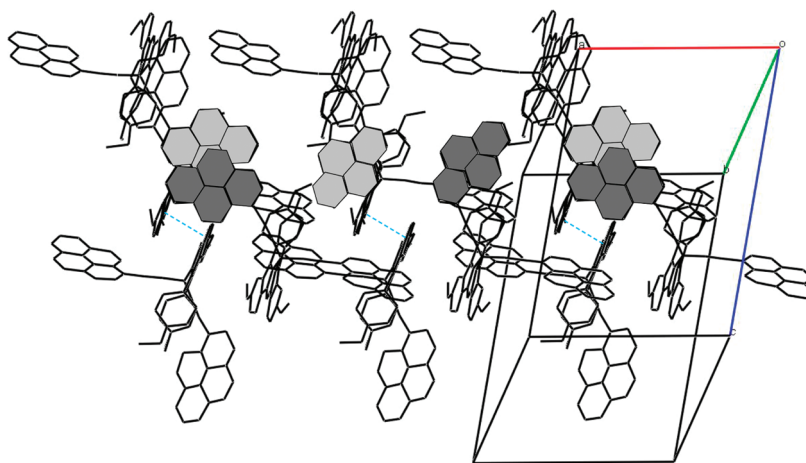


Figure 9. Packing of compound **11**. Cyan dashed lines indicate π – π stacking interactions between diisoindolemethene platforms related by inversion. Ethynylpyrene rings are colored in light and dark gray to underline the alternate positions with occupancy factors of 0.5 taken along the *a* axis. Therefore, pyrene stacking is observed every two *a* unit cell dimensions.

The electron-rich polyaromatic units seem to facilitate this second oxidation, in contrast with the alkyl substituent which does not significantly perturb the process. However, the substitution of the fluoro groups renders the first reduction more difficult by about 200 mV for an alkyne substitution and by 470 mV for an alkyl substitution (dye **14**). An intermediate situation is found for dye **15** bearing an ethynylpyrene and an ethyl fragment. In all cases, the first electrochemical reduction remains reversible and mono-electronic just like the first oxidation wave.

As would be expected based on the increase of electron density, substitution of the fluoro groups by arylethynyl fragments perturbs the second reduction of the Bodipy core, which is more cathodic by at least 140 mV. This reduction potential is located around -1.91 V and does not depend on the nature of the polyaromatic rings, excluding the direct reduction of the aryl to the radical anion [compare dye **7** (pyrenylethynyl) with dye **8** (phenylethynyl)]. Furthermore, this redox potential is shifted to -1.96 V for dye **15** (bearing pyrenylethynyl and ethyl groups) and to -2.20 V in the case of dye **14** (with two ethyl groups). The same trends are seen in the series constructed from dye **6b** with an anisole fragment and dye **6c** with an unsubstituted phenyl group (for details see Table 3).

These observations reflect the different electronic environments of Bodipy dyes and indicate that significant electronic interactions may result from substitution of the isoindole core. They clearly reflect the combined effects of electron donation of the thiophene and anisole fragments and the polyaromatic moieties grafted onto the boron center.

Optical Properties. Spectroscopic data relevant to the present discussion are collected in Table 4. In solution, all the compounds show a strong $S_0 \rightarrow S_1$ (π – π^*) transition between $\lambda \approx 630$ – 720 nm with an absorption coefficient of $80\,000$ – $120\,000$ $M^{-1} \text{ cm}^{-1}$, unambiguously assigned to the boradiisoindolemethene chromophores (Figure 11). The spectral profile is slightly dependent on the solvent polarity, and in using dioxane, dichloromethane or ethanol shifts of only a few nanometers were observed. The absorption wavelength of this band is directly affected by the level of delocalization of the boradiaindane π – π^* system and also dependent on the free rotation ability of the aromatic substituent in the ortho position to the nitrogen atoms. For instance, in the compounds where bulky substituents are present on the boron,

Table 3. Solution Electrochemical Properties of the Dyes^a

comps	E_{ox} V (ΔE , mV)		E_{red} V (ΔE , mV)	
	Bodipy ⁺ /Bodipy	Bodipy ²⁺ /Bodipy ⁺	Bodipy/Bodipy ⁻	Bodipy/Bodipy ²⁻
6a	0.43(70)	1.03 (70)	-0.92 (70)	-1.77 (irr.)
7	0.40 (80)	0.97 (irr.)	-1.10 (80)	-1.91 (irr.)
8	0.41 (70)	0.97 (irr.)	-1.12 (80)	-1.91 (irr.)
9	0.40 (80)	0.97 (irr.)	-1.11 (80)	-1.91 (irr.)
10	0.41 (70)	0.98 (irr.)	-1.11 (80)	-1.92 (irr.)
14	0.42 (80)	1.05 (90)	-1.39 (90)	-2.20 (irr.)
15	0.40 (80)	0.96 (irr.)	-1.25 (70)	-1.96 (irr.)
20a	0.40 (80)	0.98 (irr.)	-1.12 (80)	-1.92 (irr.)
6b	0.50 (70)	1.17 (80)	-1.08 (70)	-1.99 (irr.)
11	0.44 (70)	1.16 (irr.)	-1.20 (70)	-1.96 (irr.)
12	0.44 (70)	1.15 (irr.)	-1.25 (70)	-1.98 (irr.)
20b	0.42 (60)	1.18 (irr.)	-1.27 (100)	-2.00 (irr.)
6c	0.73 (70)	1.59 (irr.)	-1.06 (80)	-1.90 (irr.)
13	0.65 (80)	1.44 (irr.)	-1.27 (80)	-1.98 (irr.)
16	0.66 (60)	1.34 (irr.)	-1.29 (80)	-1.97 (irr.)
20c	0.64 (80)	1.37 (irr.)	-1.27 (80)	-1.90 (irr.)

^a Potentials determined by cyclic voltammetry in deoxygenated CH₂Cl₂ solution, containing 0.1 M TBAPF₆, at a solute concentration of ca. 1 mM and at rt. Potentials are given versus the saturated calomel electrode (SCE) and in the case of the series 6c standardized vs ferrocene (Fc) as internal reference assuming that $E_{1/2}(\text{Fc}/\text{Fc}^+) = +0.38 \text{ V}$ ($\Delta E_p = 70 \text{ mV}$) vs SCE. The error in half-wave potentials is $\pm 15 \text{ mV}$. Where the redox processes are irreversible, the peak potentials (E_{ap} or E_{cp}) are quoted. All reversible redox steps result from one-electron processes unless otherwise specified.

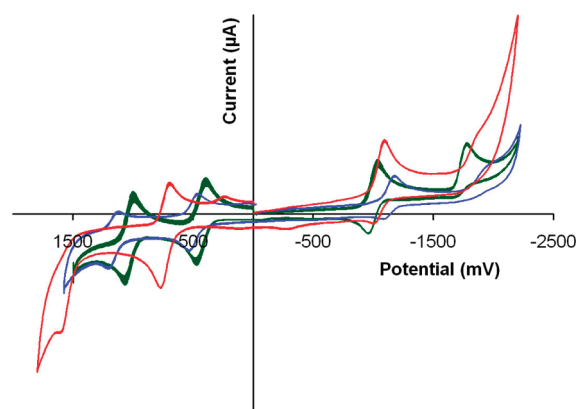
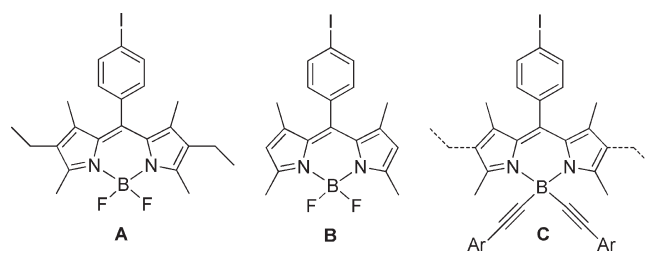


Figure 10. Cyclic voltammograms of 6a (green line), 6b (blue line), and 6c (red line) in dichloromethane at rt, using tetrabutylammonium hexafluorophosphate as the supporting electrolyte. Potentials are plotted against the saturated calomel electrode (SCE).

coplanarity of the 3,5-aryl substituents with the cyanine core is disfavored, and as a consequence the absorption is hypsochromically shifted by 91 and 52 nm (cases 14 and 15) with respect to 6a (Figure 11a). Conversely, the use of ethyne tethers or fluoro groups reduces the steric congestion, and the absorption profile is bathochromically shifted by 66 nm in the case of 8 with respect to dye 14. Interestingly, a correlation can be made between the dihedral angle between the boradiisindole plane and that of the aromatic substituents α to the nitrogen atom (see Table 2) with the observed color of the dyes. For a given diisindolomethene skeleton bearing the bulkier substituents on the boron (two ethyl groups in 14), the absorption lies at 641 nm, and the dihedral angle between the cyanine core and the thienyl group is ca. 80°. When an ethyl group is replaced by an arylethynyl substituent,

Chart 1. Nonconjugated Bodipy Dyes with Various Substituents on the Core and the Boron Atom



the dihedral angle is smaller (ca. 64°), and the delocalization pathway in the dye is enhanced, leading to an absorption at 680 nm in dye 15. With two tolylethynyl substituents (dye 8), the steric congestion around the boron is weaker (dihedral angle dye/thienyl about 54°), and a bathochromic shift is observed with an absorption located at 707 nm. With two fluorine atoms (dye 6a), the red shift is even stronger ($\lambda_{\text{abs}} = 732 \text{ nm}$). Similar conclusions apply for compounds 6c and 16, where the dihedral angle between the phenyl group and the cyanine is around 55° in the solid state structure of 6c but becomes larger (ca. 65° in the solid structure of 16) where a single ethyl group is present on the boron center. In this case, a hypsochromic shift from 634 to 612 nm is observed for the S_0-S_1 transition. Interestingly, the use of an ethynyl tether to connect an even bulkier polyaromatic group such as pyrene or perylene to the boron atom does not dramatically affect the color of the dye with respect to the reference difluoro compounds. There is an apparent correlation between the dihedral angles observed crystallographically in the molecular structures and the spectroscopic data; however, we have to keep in mind that these dihedral angles are not fixed in solution, and the electronic as well as steric effects of the substituents may be significantly different in both

Table 4. Spectroscopic Data for the Compounds at 298 K^a

compds	λ_{abs} (nm)	ϵ (M ⁻¹ cm ⁻¹)	λ_{F} (nm)	Φ_{F}^b (%)	P_{ET}^c	τ_{F} (ns)	k_{r}^d (10 ⁷ s ⁻¹)	k_{nr}^d (10 ⁷ s ⁻¹)	Stokes shift (cm ⁻¹)
6a	732	77800	780	16		2.6	6.35	32.1	840
7	720	78100	756	21		5.3	3.96	14.9	660
	370	1117000		21	100				13800
8	707	85000	746	29		7.5	3.9	9.5	740
9	720	82000	755	24		4.6	5.2	16.5	644
	464	117000	755	15	63		3.2	18.5	8307
			496	4					1390
10	709	82000	750	22		5.2	4.2	15.0	771
	324	110000		16	72		3.1	16.2	17530
14	641	91200	697	43		5.4	7.9	10.6	1250
15	680	78000	737	26		5.3	4.9	14.0	1137
	371	70000		20	77		3.8	15.1	13386
20a	717	79000	753	24		4.7	5.1	16.2	631
	371	76000		24			5.1	16.2	13700
21a	716	83000	751	19		5.4	3.5	15.0	650
	371	79000		17	89		3.1	15.4	13700
22a	713	84000	750	24		5.2	4.6	14.6	692
	371	101500		21	88		4.1	15.2	13600
6b	679	89800	708	49		6.8	7.2	7.5	603
11	669	84500	695	52		6.9	7.5	6.9	560
	370	102000		52	100		7.5	6.9	12638
12	668	76100	700	49		7.5	6.5	6.8	684
20b	671	89800	701	57		7.4	7.7	5.8	638
	368	73200		57	100		7.7	5.8	12910
21b	669	75800	701	50		6.4	7.8	7.8	682
	368	54000		49	98		7.6	7.9	12910
6c	641	103700	663	65		6.6	9.8	5.3	518
13	632	82500	656	60		9.6	6.2	4.2	479
16	612	94100	643	71		6.2	11.5	4.7	788
	370	46700		70	99		11.3	4.8	11475
20c	634	82900	658	62		8.2	7.6	4.6	575
	368	52600		61	98		7.4	4.8	11976
21c	634	92300	660	65		6.4	10.2	5.5	621
	368	55100		64			10.0	5.6	12000

^a Measured in CH₂Cl₂ at 25 °C. ^b Determined in dichloromethane solution, ca. 5 × 10⁻⁷ M. Using Cresyl Violet, as reference ($\phi_{\text{F}} = 0.50$ in ethanol)⁴² and compounds ($\phi_{\text{F}} = 0.51$ in methanol) **6b**.^{22a} All Φ_{F} are corrected for changes in refractive index. ^c Energy transfer efficiency calculated by dividing the photoluminescence quantum yield obtained by irradiation in the aryl fragment by the yield obtained by direct excitation in the S₁ transition. ^d Calculated using the following equations: $k_{\text{r}} = \Phi_{\text{F}} / \tau_{\text{F}}$, $k_{\text{nr}} = (1 - \Phi_{\text{F}}) / \tau_{\text{F}}$, assuming that the emitting state is produced with unit quantum efficiency.

situations. Similar observations were recently reported for *F*-Bodipys bearing various aromatic substituents on the 3,5-positions.³⁵ Other spectroscopic characteristics are the broad bands observed in the 350–420 nm window corresponding to the S₀→S₂ (π - π^*) transition³⁶ of the boradiazaindacene. We have previously noted that the S₀→S₂ transition of extended Bodipys is not shifted significantly by increasing the delocalization pathway.³⁷ The polyaromatic fragments introduce strong π - π^* transitions with marked vibronic structure at 320–370 and 230–310 nm for pyrene,³⁸ 250–340 nm for fluorene,³⁹ and 400–480 nm for perylene.⁴⁰ The absorption envelope in the 350–420 nm window of compounds **7–11** and **15–22a** can be analyzed as a superposition of the separate absorptions of the boradiazaindacene and the polyaromatic fragments. This observation confirms that each module remains isolated and that delocalization over the Bodipy core and the polyaromatic fragments is not effective. This result is in keeping with the absence of available orbitals on the boron(III) center.

Excitation of all the compounds in the S₀→S₁ transition present in the 632–727 nm range leads to emission in the region 640–780 nm, and the small Stokes shifts observed indicate that the fluorescence originates from a weakly polarized state in which little reorganization is occurring (Figure 11b). The relatively high quantum yield values observed for the red emitters decrease as the emitting wavelength energy decreases, in keeping with the energy gap law, from 65% for **6c** to 16.5% for **6a** (Table 4).⁴¹ The fluorescence decay profiles can be described by a single exponential fit, with fluorescence lifetimes in the range of 3–9 ns, a result in accordance with a singlet excited state. In fact, the radiative rate constants are much faster than the nonradiative rate constants for compounds emitting below 680 nm, indicating minimal interaction of the emitting state with an energetically low-lying localized state (triplet, charge transfer states, or vibronic energy loss) reflected in the high quantum yields. For compounds emitting in the NIR region, the nonradiative rate constant is higher than the

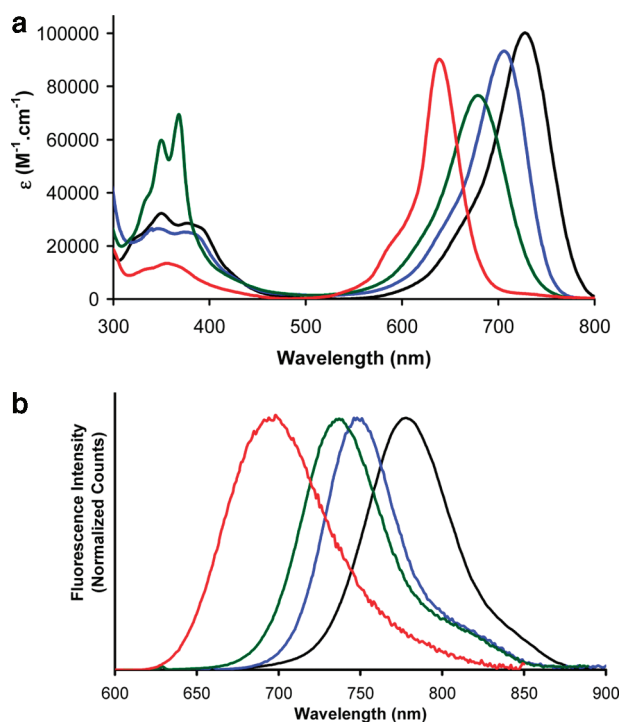


Figure 11. (a) Absorption spectra of **6a** (black line), **8** (blue line), **15** (green line), and **14** (red line) in dichloromethane at rt. (b) Emission spectra of **6a** (black line), **8** (blue line), **15** (green line), and **14** (red line) in dichloromethane at rt (excitation in the respective S_0 – S_1 absorption band, respectively, at 700, 660, 630, and 595 nm).

radiative one. No significant solvatochromic effect was observed in the absorption and fluorescence spectra, confirming weak polarization of the ground and excited states which is also in keeping with a singlet excited state.

For compounds **7**–**11**, **15**, **16**, and **20**–**22**, excitation in the most intense absorption band of the polyaromatic fragments (250–470 nm range) did show weak residual emission of the polycyclic fragments and the characteristic emission of the boradiazaindacene core (Figure 12 and Figures S67, S69, S74, and S76–82, Supporting Information). In all cases, the fluorescence excitation spectra match the absorption spectra, confirming a very efficient energy transfer from the polyaromatic parts to the indacene emitter (Figure 13 and Figure S64–S83, Supporting Information). The quantum yield measurements are in agreement with an intramolecular energy transfer efficiency of 70–100% (calculated by dividing the photoluminescence quantum yield obtained by irradiation in the aryl fragment by the yield obtained by direct excitation in the S_1 transition). The efficiency of the energy transfer is likely due to a good overlap of the S_0 → S_2 band of the boradiazaindacene emitter with the emission band of the pyrene and fluorene unit leading to a very efficient Förster-type energy transfer, as we have previously observed with the pyrene-substituted Bodipy dyad^{19d} and polychromophoric systems based on the compound **6a** skeleton bearing multiple phenyl-ethynyl-polyaromatic on the boron center.³⁶ In the case of compound **9**, a weak overlap between perylene emission and S_0 → S_1 transition takes place; the energy transfer is less efficient and a residual emission of 4% of the perylene could be observed (Figure 12b).

Compounds bearing the same antenna (e.g., pyrene in **7**, **11**, and **16**) on the boron form a model family of Red-NIR dyes having a common excitation wavelength and different emission

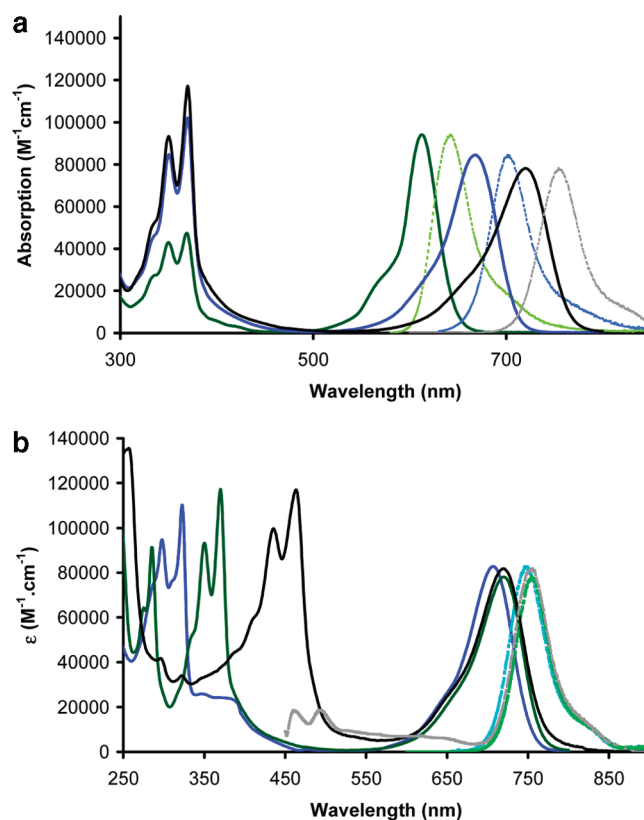


Figure 12. (a) Absorption (full lines) and emission spectra (dotted lines, excitation in the high-energy polyaromatic band, $\lambda = 360$ nm) of **7** (black), **11** (blue), and **16** (green) in dichloromethane, at rt. (b) Absorption (dark lines) and emission spectra (light lines, excitation in the high-energy polyaromatic band) of **9** (black), **7** (blue), and **10** (green) in dichloromethane, at rt.

band (Figure 12a). This interesting feature is maintained even within the series of compounds possessing a benzoate group (**21**) and for the product **22a** of coupling to a primary amine.

CONCLUSION

By using diisoindolomethene-based Bodipy dyes bearing various substituents on the core (ethylthiophene, anisole, or phenyl rings), we have been able to build efficient cassette systems after introduction of 1-ethynylpyrene or 3-ethynylperylene units on the boron center by means of Grignard reagents. The simultaneous addition of two different carbanions during the substitution reaction gave us the opportunity to construct several boron-centered heterodisubstituted systems. This has provided dyes with pyrene as a high-energy input unit and an activated acid function allowing grafting on various supports. Steric hindrance around the boron center is a means of tuning the absorption and emissive properties. In particular, bulky groups tethered on the boron induce a pronounced rotation of the substituents *ortho* to the nitrogen atoms, reducing the delocalization pathway and resulting in a pronounced hypsochromic shift of about 91 nm compared to the difluoro starting material. The pyrene residue can be used as an input energy module promoting very efficient intramolecular energy transfer to the Bodipy subunit, which then emits the light absorbed by the pyrene. This is also true for perylene substituents. In these two cases, Stokes shifts of around 13 000 and 8000 cm^{-1} ,

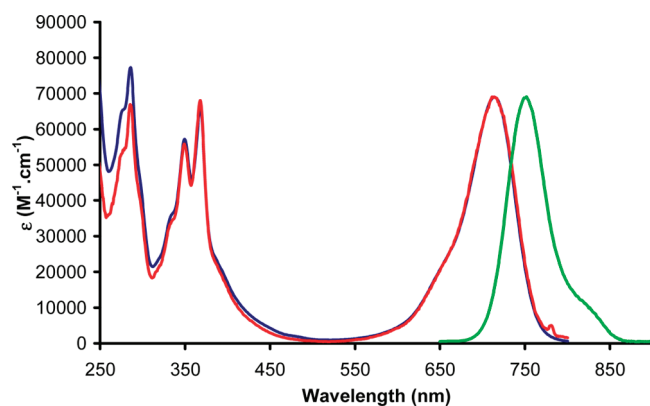


Figure 13. Absorption (blue line), emission (green line, λ_{exc} 380 nm), and excitation (red line, λ_{em} 780 nm) spectra of **20a**.

respectively, were obtained. In the extreme case of a functionalized fluorene, the value reached $17\,500\text{ cm}^{-1}$.

Finally, these dyes are redox active, exhibiting reversible reduction and oxidation to the radical cation and radical anion. In some cases, further reduction to the dication and dianion is also readily observed. To obtain red-NIR emitters suitable for biological labeling, the next step is to balance the hydrophobic character of these new dyes by decoration with hydrophilic groups, such as the charged groups recently used to obtain water-soluble Bodipys emitting in the 500–600 nm window.⁴³ We are currently investigating different approaches to gain water solubility and thus emissive dyes suitable for use in biological conditions and for bioconjugation to vitamins, polypeptides, sugars, native or modified proteins, and antibodies.

EXPERIMENTAL SECTION

Ethyl 5-Ethylthiophene-2-carboxylate (1a): to a solution of 2-ethylthiophene (10.00 g, 89.13 mmol) in THF (70 mL) at $-78\text{ }^{\circ}\text{C}$ was added dropwise *n*-butyllithium (65 mL, 97.50 mmol, 1.50 M in hexanes). The solution was stirred for 1 h and added via a cannula to a solution of ethyl chloroformate (9.7 mL, 106.96 mmol) in THF (50 mL). The mixture was stirred at $-78\text{ }^{\circ}\text{C}$ for 1 h and quenched with a saturated solution of NH_4Cl (100 mL). The aqueous layer was extracted with dichloromethane. The organic extracts were washed with water and brine and dried over magnesium sulfate. The solvent was removed by rotary evaporation. The residue was purified by chromatography on silica gel, eluting with dichloromethane–cyclohexane (v/v 60/40) to give 14.71 g (89%) of **1a** as a colorless viscous liquid. $^1\text{H NMR}$ (200 MHz, CDCl_3): δ 7.61 (d, 1H, $^3J = 3.6\text{ Hz}$), 6.78 (dt, 1H, $^3J = 3.6\text{ Hz}$, $^4J = 1.1\text{ Hz}$), 4.31 (q, 2H, $^3J = 7.3\text{ Hz}$), 2.85 (q, 2H, $^3J = 7.3\text{ Hz}$), 1.35 (t, 3H, $^3J = 7.3\text{ Hz}$), 1.31 (t, 3H, $^3J = 7.3\text{ Hz}$). $^{13}\text{C NMR}$ (50 MHz, CDCl_3): δ 162.3, 155.3, 133.5, 130.9, 124.4, 60.8, 23.8, 15.6, 14.3. ES-MS m/z (nature of the peak, relative intensity) 185.2 ($[\text{M} + \text{H}]^+$, 100), 140.2 ($[\text{M} - \text{OEt}]^+$, 20). Anal. Calcd for $\text{C}_9\text{H}_{12}\text{O}_2\text{S}$: C, 58.67; H, 6.56. Found: C, 58.41; H, 6.40%.

5-Ethylthiophene-2-carbohydrazide (2a): to a solution of **1a** (14.00 g, 75.98 mmol) in EtOH (30 mL) was added dropwise hydrazine monohydrate (11 mL, 227.94 mmol). The mixture was refluxed for 12 h, and then the solvent was removed by rotary evaporation. The residue was treated with water and extracted with dichloromethane. The organic extracts were washed with water and brine and dried over magnesium sulfate. The solvent was removed by rotary evaporation. The residue was purified by recrystallization from warm cyclohexane to give 8.90 g (69%) of **2a** as a white solid: mp $87\text{--}88\text{ }^{\circ}\text{C}$. $^1\text{H NMR}$ (200 MHz, CDCl_3): δ 7.38 (d, 1H, $^3J = 3.6\text{ Hz}$), 6.77 (dt, 1H, $^3J = 3.6\text{ Hz}$, $^4J = 1.1\text{ Hz}$), 3.99 (s, 2H), 2.85 (qd, 2H, $^3J = 7.3\text{ Hz}$, $^4J =$

1.1 Hz), 1.31 (t, 3H, $^3J = 7.3\text{ Hz}$). $^{13}\text{C NMR}$ (50 MHz, CDCl_3): δ 163.5, 153.2, 133.1, 128.8, 124.3, 23.6, 15.6. ES-MS m/z (nature of the peak, relative intensity) 171.2 ($[\text{M} + \text{H}]^+$, 100), 139.2 ($[\text{M} - \text{NHNH}_2]^+$, 20). Anal. Calcd for $\text{C}_7\text{H}_{10}\text{N}_2\text{O}_2\text{S}$: C, 40.76; H, 6.84; N, 13.58. Found: C, 40.55; H, 6.77; N, 13.37%.

(E)-5-Ethyl-*N'*-(1-(2-hydroxy-4-methoxyphenyl)ethylidene)-thiophene-2-carbohydrazide (3a): a mixture of **2a** (2.90 g, 17.04 mmol) and 2-hydroxy-4-methoxyacetophenone (2.83 g, 17.04 mmol) was stirred without solvent at $75\text{ }^{\circ}\text{C}$ for 1 h. The resulting yellowish solid was purified by recrystallization from a mixture of dichloromethane and methyl alcohol to give 4.52 g (87%) of **3a** as a white solid: mp $110\text{--}111\text{ }^{\circ}\text{C}$. $^1\text{H NMR}$ (200 MHz, CDCl_3): δ 9.18 (s, 1H), 7.52 (s, 1H), 7.29 (d, 1H, $^3J = 8.2\text{ Hz}$), 6.72 (d, 1H, $^3J = 3.6\text{ Hz}$), 6.43–4.34 (m, 2H), 3.75 (s, 3H), 2.80 (q, 2H, $^3J = 7.5\text{ Hz}$), 2.31 (s, 3H), 1.27 (t, 3H, $^3J = 7.5\text{ Hz}$). $^{13}\text{C NMR}$ (50 MHz, CDCl_3): δ 162.3, 161.1, 156.4, 154.4, 132.9, 132.2, 129.9, 129.0, 124.6, 112.5, 106.3, 101.8, 55.3, 23.7, 15.6, 12.8. ES-MS m/z (nature of the peak, relative intensity) 319.2 ($[\text{M} + \text{H}]^+$, 100). Anal. Calcd for $\text{C}_{16}\text{H}_{18}\text{N}_2\text{O}_3\text{S}$: C, 57.12; H, 5.99; N, 8.33. Found: C, 56.81; H, 5.73; N, 8.19%.

(5-ethyl-2-thienyl)(2-acetyl-5-methoxy-1-phenyl) ketone (4a): to a solution of **3a** (4.30 g, 14.15 mmol) in THF (150 mL) was added slowly at $25\text{ }^{\circ}\text{C}$ $\text{Pb}(\text{OAc})_2$ (7.52 g, 16.96 mmol). After 1 h the solution was filtered, and the solvent was removed by rotary evaporation. The residue was treated with water and extracted with dichloromethane. The organic extracts were washed with water and brine and dried over magnesium sulfate. The solvent was removed by rotary evaporation. The residue was purified by chromatography on alumina, eluting with dichloromethane–cyclohexane (v/v 40/60) to give 4.01 g (98%) of **4a** as a white solid: mp $69\text{--}70\text{ }^{\circ}\text{C}$. $^1\text{H NMR}$ (200 MHz, CDCl_3): δ 7.83 (d, 1H, $^3J = 8.6\text{ Hz}$), 7.06 (d, 1H, $^3J = 3.7\text{ Hz}$), 6.98 (dd, 1H, $^3J = 8.6\text{ Hz}$, $^4J = 2.5\text{ Hz}$), 6.88 (d, 1H, $^4J = 2.5\text{ Hz}$), 6.72 (dd, 1H, $^3J = 3.7\text{ Hz}$, $^4J = 0.8\text{ Hz}$), 3.84 (s, 3H), 2.84 (q, 2H, $^3J = 7.3\text{ Hz}$), 2.46 (s, 3H), 1.29 (t, 3H, $^3J = 7.8\text{ Hz}$). $^{13}\text{C NMR}$ (50 MHz, CDCl_3): δ 196.3, 189.3, 162.4, 157.6, 142.8, 141.4, 134.2, 131.8, 129.2, 124.7, 114.2, 113.6, 55.6, 27.0, 23.9, 15.3. ES-MS m/z (nature of the peak, relative intensity) 289.1 ($[\text{M} + \text{H}]^+$, 100). Anal. Calcd for $\text{C}_{16}\text{H}_{16}\text{O}_3\text{S}$: C, 66.64; H, 5.59. Found: C, 66.41; H, 5.35%.

Compound 5a: to a solution of **4a** (330 mg, 1.14 mmol) in acetic acid (2.4 mL) and ethyl alcohol (12 mL) at $65\text{ }^{\circ}\text{C}$ was added ammonium acetate (536 mg, 6.87 mmol) and ammonium chloride (61 mg, 1.14 mmol). The solution was then refluxed at $90\text{ }^{\circ}\text{C}$ for 30 min. The solvent was removed by rotary evaporation. The residue was treated with water and extracted with dichloromethane. The organic extracts were washed with water and dried over absorbent cotton. The solvent was removed by rotary evaporation. The residue was purified by chromatography on silica gel, eluting with dichloromethane to give 149 mg (50%) of **5a** as a deep blue solid: $166\text{ }^{\circ}\text{C}$ (dec). $^1\text{H NMR}$ (400 MHz, $\text{CDCl}_3\text{--CCl}_4$ (v/v 50/50)): δ 7.61 (d, 2H, $^3J = 8.5\text{ Hz}$), 7.46 (s, 2H), 7.21 (s, 2H), 7.06 (s, 1H), 6.86 (m, 4H), 3.91 (s, 6H), 2.98 (q, 4H, $^3J = 7.3\text{ Hz}$), 1.46 (t, 6H, $^3J = 7.4\text{ Hz}$). $^{13}\text{C NMR}$ (100 MHz, CDCl_3): δ 158.1, 148.3, 140.1, 135.5, 133.8, 130.8, 129.7, 124.8, 124.7, 120.2, 117.2, 109.2, 102.4, 55.3, 24.0, 16.2. UV–vis (CH_2Cl_2): λ nm (ϵ , $\text{M}^{-1}\text{ cm}^{-1}$) 359 (33000), 659 (48000). ES-MS m/z (nature of the peak, relative intensity) 525.2 ($[\text{M} + \text{H}]^+$, 100). Anal. Calcd for $\text{C}_{31}\text{H}_{28}\text{N}_2\text{O}_2\text{S}_2 \cdot \text{H}_2\text{O}$: C, 68.61; H, 5.57; N, 5.16. Found: C, 68.33; H, 5.27; N, 5.03%.

Compound 3b: 4-Methoxyphenyl-1-carbohydrazide (**2b**) (4.00 g, 24.01 mmol) and 2-hydroxy-4-methoxyacetophenone (4.00 g, 24.01 mmol) were stirred in refluxing *n*-propanol overnight. After cooling, the solid is filtered and recrystallized from boiling *n*-propanol, giving 5.10 g (67%) of pure **3b** as a white solid. $^1\text{H NMR}$ (200 MHz, $\text{DMSO-}d_6$): δ 13.71 (s, 1H), 11.07 (s, 1H), 7.49 (ABsys, 4H, $J_{\text{AB}} = 9.0\text{ Hz}$, $\nu\delta_{\text{AB}} = 170.3\text{ Hz}$), 7.54 (d, 1H, $^3J = 9.3\text{ Hz}$), 6.45–6.50 (m, 2H), 3.84 (s, 3H), 3.77 (s, 3H), 2.43 (s, 3H). $^{13}\text{C NMR}$ (50 MHz, $d_6\text{-DMSO}$): δ 163.5, 162.1, 161.6, 160.7, 158.0, 129.9, 129.6, 124.9, 113.6, 112.7, 105.5, 101.5,

55.4, 55.1, 13.9. IR (KBr): 3429, 3253, 2835, 1634, 1615, 1597, 1493, 1254, 1181, 1022, 830 cm^{-1} . ES-MS m/z (nature of the peak, relative intensity) 315.1 ($[\text{M} + \text{H}]^+$, 100). Anal. Calcd for $\text{C}_{17}\text{H}_{18}\text{N}_2\text{O}_4$: C, 64.96; H, 5.77; N, 8.91. Found: C, 64.78; H, 5.55; N, 8.76%.

Compound 4b: to a solution of compound **3b** (7.00 g, 22.27 mmol) in THF (170 mL) was added slowly at 25 °C $\text{Pb}(\text{OAc})_4$ (11.84 g, 26.72 mmol). After 1 h the solution was filtered, the solid extracted with dichloromethane, and the final organic layer evaporated to dryness. The residue was extracted with dichloromethane and washed with water and brine and dried over magnesium sulfate. The residue was purified by chromatography (alumina Act IV, dichloromethane/cyclohexane 40:60) to give 4.13 g (65%) of **4b** as a white solid. ^1H NMR (300 MHz, CDCl_3): δ 7.88 (d, 1H, $^3J = 8.7$ Hz), 7.31 (ABsys, 4H, $J_{\text{AB}} = 8.8$ Hz, $\nu_{\text{AB}} = 248.0$ Hz), 7.02 (dd, 1H, $^3J = 8.7$ Hz, $^4J = 2.4$ Hz), 6.85 (d, 1H, $^4J = 2.4$ Hz), 3.88 (s, 3H), 3.85 (s, 3H), 2.47 (s, 3H). ^{13}C NMR (75 MHz, CDCl_3): δ 196.2, 196.1, 163.3, 162.7, 143.9, 131.8, 131.3, 130.0, 129.2, 114.1, 113.6, 113.3, 55.6, 55.4, 26.7. IR (KBr): 2942, 2844, 1670, 1654, 1600, 1567, 1422, 1261, 1174, 1023, 823 cm^{-1} . ES-MS m/z (nature of the peak, relative intensity) 285.1 ($[\text{M} + \text{H}]^+$, 100). Anal. Calcd for $\text{C}_{17}\text{H}_{16}\text{O}_4$: C, 71.82; H, 5.67. Found: C, 71.67; H, 5.40%.

Compound 5b: to a solution of compound **4b** (2.70 g, 9.5 mmol) in acetic acid (60 mL) and methanol (120 mL) was added dropwise NH_4OH (35 mL). After addition completion, the solution was stirred at RT for one day. The blue precipitate was filtered and then dissolved in chloroform. The blue organic solution was then washed with water (3×30 mL) and dried over MgSO_4 . Chromatography (SiO_2 , dichloromethane) gave **5b** as a deep blue solid (1.30 g, 53%). ^1H NMR (300 MHz, CDCl_3 - CCl_4 (v/v 50/50)): δ 7.90 (br d, 4H, $^3J = 7.9$ Hz), 7.72 (br d, 2H, $^3J = 8.8$ Hz), 7.22–7.29 (br s, 3H), 7.07 (d, 4H, $^3J = 8.8$ Hz), 6.96 (dd, 2H, $^3J = 8.7$ Hz, $^4J = 2.2$ Hz), 3.93 (s, 6H), 3.90 (s, 6H). ^{13}C NMR (75 MHz, CDCl_3 - CCl_4 (v/v 50/50)): δ 157.7, 128.7, 128.6, 120.2, 116.9, 114.6, 102.5, 55.5, 55.4. ES-MS m/z (nature of the peak, relative intensity) 517.2 ($[\text{M} + \text{H}]^+$, 100). Anal. Calcd for $\text{C}_{33}\text{H}_{28}\text{N}_2\text{O}_4$: C, 76.73; H, 5.46; N, 5.42. Found: C, 76.53; H, 5.20; N, 5.37%.

Compound 5c: to a solution of **4c**²⁵ (10.00 g, 44 mmol) in acetic acid (200 mL) and methanol (400 mL) was added dropwise concentrated aqueous ammonia (100 mL). After addition was complete, the solution was stirred at RT for one day, while the solution turned progressively deep blue. The blue precipitate was filtered and then dissolved in chloroform. The blue organic solution was then washed with water (3×30 mL) and dried over MgSO_4 . Chromatography (SiO_2 , chloroform) gave **5c** as a deep blue solid (6.50 g, 74%). ^1H NMR (300 MHz, CDCl_3): δ 8.01–8.06 (m, 6H), 7.92 (d, 2H, $^3J = 8.1$ Hz), 7.59–7.54 (m, 5H), 7.47–7.43 (m, 2H), 7.38–7.35 (m, 2H), 7.32–7.29 (m, 2H). ^{13}C NMR (75 MHz, CDCl_3): δ 146.8, 136.2, 133.8, 133.3, 129.2, 129.1, 128.6, 127.5, 126.2, 124.8, 119.2, 111.2, 111.8. ES-MS m/z (nature of the peak, relative intensity) 397.2 ($[\text{M} + \text{H}]^+$, 100). Anal. Calcd for $\text{C}_{29}\text{H}_{20}\text{N}_2$: C, 87.85; H, 5.08; N, 7.07. Found: C, 87.77; H, 4.99; N, 6.98%.

General Procedure Following Experimental Conditions 1 to Produce the BODIPY 6a–c. To a solution of compounds **5a–c** in anhydrous dichloromethane were added dropwise successively *N,N*-diisopropylethylamine and boron trifluoride-diethyl etherate. The mixture was stirred at room temperature until the complete consumption of the starting material (determined by TLC), and then water was added. The organic extracts were washed with water and dried over hydrophilic cotton. The solvent was removed by rotary evaporation. The residue was purified by chromatography on silica gel, eluting with dichloromethane

Compound 6a. Compound **5a** (880 mg, 1.68 mmol), anhydrous dichloromethane (110 mL), *N,N*-diisopropylethylamine (650 mg, 5.03 mmol), and boron trifluoride-diethyl etherate (1.43 g, 10.06 mmol). 773 mg (81%) of compound **6a** was obtained as a deep green solid: mp 277–278 °C. ^1H NMR (400 MHz, CDCl_3 - CCl_4 (v/v 50/50)): δ 7.85 (s, 2H), 7.64 (d, 2H, $^3J = 9.0$ Hz), 7.39 (s, 1H), 7.29 (s, 2H), 6.98 (m, 4H), 3.86 (s, 6H), 2.98 (q, 4H, $^3J = 7.5$ Hz), 1.43 (t, 6H, $^3J = 7.5$ Hz). ^{13}C NMR (100 MHz,

CDCl_3 - CCl_4 (v/v 50/50)): δ 158.3, 151.6, 132.0, 131.4, 129.8, 128.9, 125.1, 120.8, 120.2, 103.1, 55.5, 23.7, 15.6. ^{11}B NMR (128 MHz, CDCl_3 - CCl_4 (v/v 50/50)): 5.15 (s). UV-vis (CH_2Cl_2): λ nm (ϵ , $\text{M}^{-1} \text{cm}^{-1}$) 353 (29000), 380 (25000), 650 (sh, 21000), 727 (90000). ES-MS m/z (nature of the peak, relative intensity) 573.2 ($[\text{M} + \text{H}]^+$, 100), 534.2 ($[\text{M} - 2\text{F}]^+$, 35). Anal. Calcd for $\text{C}_{31}\text{H}_{27}\text{BF}_2\text{N}_2\text{O}_2\text{S}_2$: C, 65.04; H, 4.75; N, 4.89. Found: C, 64.92; H, 4.62; N, 4.74%.

Compound 6b. Compound **5b** (0.705 g, 1.37 mmol), anhydrous dichloromethane (150 mL), *N,N*-diisopropylethylamine (0.7 mL, 4.11 mmol), and boron trifluoride-diethyl etherate (1 mL, 11.62 mmol). 700 mg (88%) of compound **6b** was obtained as deep blue needles. ^1H NMR (300 MHz, CDCl_3 - CCl_4 (v/v 50/50)): δ 7.90 (br d, 4H, $^3J = 7.9$ Hz), 7.72 (br d, 2H, $^3J = 8.9$ Hz), 7.28 (br s, 3H), 7.06 (d, 4H, $^3J = 8.9$ Hz), 6.96 (dd, 2H, $^3J = 8.7$ Hz, $^4J = 2.2$ Hz), 3.93 (s, 6H), 3.91 (s, 6H). ^{11}B NMR (128 MHz, CDCl_3 - CCl_4 (v/v 50/50)): 5.00 (t, $J = 31.9$ Hz). UV-vis (CH_2Cl_2): λ nm (ϵ , $\text{M}^{-1} \text{cm}^{-1}$) 367 (19200), 679 (89800). ES-MS m/z (nature of the peak, relative intensity) 565.2 ($[\text{M} + \text{H}]^+$, 100), 545.2 ($[\text{M} - \text{F}]^+$, 25), 526.2 ($[\text{M} - 2\text{F}]^+$, 5). Anal. Calcd for $\text{C}_{33}\text{H}_{27}\text{BF}_2\text{N}_2\text{O}_4$: C, 70.23; H, 4.82; N, 4.96. Found: C, 70.07; H, 4.72; N, 4.80%.

Compound 6c. Compound **5c** (2.00 g, 5.04 mmol), anhydrous dichloromethane (50 mL), *N,N*-diisopropylethylamine (2.6 mL, 14.92 mmol), and boron trifluoride-diethyl etherate (1.9 mL, 14.92 mmol). 1.40 g (63%) of compound **6c** was isolated as a deep blue solid. ^1H NMR (200 MHz, CDCl_3): δ 7.92 (d, 2H, $^3J = 8.0$ Hz), 7.80–7.85 (m, 4H), 7.63 (d, 2H, $^3J = 8.4$ Hz), 7.43–7.50 (m, 9H), 7.21–7.28 (m, 2H). ^{13}C NMR (75 MHz, CDCl_3): δ 151.7, 134.2, 131.0, 130.6, 130.2, 129.5, 129.0, 128.2, 125.3, 123.7, 118.9, 114.8. ^{11}B NMR (128 MHz, CDCl_3): 5.10 (t, $J = 31.6$ Hz). UV-vis (CH_2Cl_2): λ nm (ϵ , $\text{M}^{-1} \text{cm}^{-1}$) 299 (30000), 340 (21700), 641 (103700). ES-MS m/z (nature of the peak, relative intensity) 445.2 ($[\text{M} + \text{H}]^+$, 100), 425.2 ($[\text{M} - \text{F}]^+$, 25). Anal. Calcd for $\text{C}_{29}\text{H}_{19}\text{BF}_2\text{N}_2$: C, 78.40; H, 4.31; N, 6.31. Found: C, 78.19; H, 4.15; N, 6.20%.

General Procedure Following Experimental Conditions 2 for the Fluoro Substitution Leading to Compounds 7–16. A Schlenk flask was charged with the ethynyl derivative (2.4 equiv) and anhydrous THF. A solution of ethylmagnesium bromide (2.2 equiv, 1 M in THF) was then added dropwise, and the mixture was stirred at 50 °C for 2 h. The mixture was then added at 25 °C via a cannula to a solution of difluoroborate complex (1 equiv) in anhydrous THF. The mixture was stirred at 70 °C for 16 h, and the solvent was removed by rotary evaporation. The residue was treated with water and extracted with dichloromethane. The organic extracts were washed with water and dried over MgSO_4 . The solvent was removed by rotary evaporation. The residue was purified by chromatography.

Compound 7. Prepared following experimental conditions 2; from **6a** (50 mg, 0.09 mmol), 4-ethynylpyrene (69 mg, 0.31 mmol), EtMgBr (0.26 mL, 0.26 mmol, 1 M in THF), THF (8 mL); chromatography on silica gel, eluting with dichloromethane–cyclohexane (v/v 40/60) to give **41** mg (46%) of **7** as a green solid: 162 °C (dec). ^1H NMR (400 MHz, CDCl_3 - CCl_4 (v/v 50/50)): 8.55 (d, 2H, $^4J = 3.6$ Hz), 8.35 (d, 2H, $^3J = 9.2$ Hz), 8.10 (m, 4H), 7.99–7.93 (m, 10H), 7.82–7.76 (m, 5H), 7.41 (s, 2H), 7.06 (dd, 2H, $^3J = 8.0$ Hz, $^4J = 2.4$ Hz), 6.91 (d, 2H, $^4J = 3.6$ Hz), 3.92 (s, 6H), 2.75 (q, 4H, $^3J = 7.4$ Hz), 1.08 (t, 6H, $^3J = 7.4$ Hz). ^{13}C NMR (100 MHz, CDCl_3 - CCl_4 (v/v 50/50)): 158.2, 151.2, 143.1, 133.6, 132.4, 132.0, 131.4, 130.5, 130.4, 129.9, 128.7, 127.6, 127.5, 127.4, 127.3, 126.8, 125.9, 125.0, 124.9, 124.62, 124.57, 124.5, 124.2, 120.4, 120.2, 119.9, 112.8, 102.9, 98.1, 55.5, 23.6, 15.5. ^{11}B NMR (128 MHz, CDCl_3 - CCl_4 (v/v 50/50)): -6.25 (s). UV-vis (CH_2Cl_2): λ nm (ϵ , $\text{M}^{-1} \text{cm}^{-1}$) 248 (127000), 275 (94000), 286 (135000), 351 (108000), 370 (141000), 661 (33000), 719 (91500). ES-MS m/z (nature of the peak, relative intensity) 985.1 ($[\text{M} + \text{H}]^+$, 100), 759.2 ($[\text{M} - \text{ethynylpyrene}]^+$, 15). Anal. Calcd for $\text{C}_{67}\text{H}_{45}\text{BN}_2\text{O}_2\text{S}_2$: C, 81.49; H, 4.60; N, 2.84. Found: C, 81.46; H, 4.28; N, 2.68%.

Compound 8. Prepared following experimental conditions 2; from **6a** (60 mg, 0.10 mmol), 4-ethynyltoluene (43 mg, 0.37 mmol), EtMgBr (0.31 mL, 0.31 mmol, 1 M in THF), THF (8 mL); chromatography on silica gel, eluting with dichloromethane–cyclohexane (v/v 40/60) to give 50 mg (62%) of **8** as a green solid: 234 °C (dec). ^1H NMR (400 MHz, $\text{CDCl}_3\text{--CCl}_4$ (v/v 50/50)): 8.32 (d, 2H, $^4J = 3.6$ Hz), 7.61 (m, 3H), 7.20 (m, 2H), 7.02–6.84 (m, 12H), 3.84 (s, 6H), 2.99 (q, 4H, $^3J = 7.4$ Hz), 2.28 (s, 6H), 1.42 (t, 6H, $^3J = 7.4$ Hz). ^{13}C NMR (100 MHz, $\text{CDCl}_3\text{--CCl}_4$ (v/v 50/50)): 157.8, 150.3, 142.7, 136.6, 133.3, 132.1, 131.5, 130.5, 128.5, 127.4, 124.7, 122.4, 119.9, 119.8, 113.1, 102.4, 98.5, 55.3, 23.7, 21.5, 15.9. ^{11}B NMR (128 MHz, $\text{CDCl}_3\text{--CCl}_4$ (v/v 50/50)): –7.29 (s). UV–vis (CH_2Cl_2): λ nm (ϵ , $\text{M}^{-1}\text{cm}^{-1}$) 257 (101000), 267 (102000), 350 (24000), 380 (23000), 645 (26000), 709 (90500). ES-MS m/z (nature of the peak, relative intensity) 765.2 ($[\text{M} + \text{H}]^+$, 100), 649.2 ($[\text{M} - \text{ethynyltoluene}]^+$, 25). Anal. Calcd for $\text{C}_{49}\text{H}_{41}\text{BN}_2\text{O}_2\text{S}_2$: C, 76.95; H, 5.40; N, 3.66. Found: C, 76.70; H, 5.12; N, 3.46%.

Compound 9. Prepared following experimental conditions 2; from **6a** (50 mg, 0.09 mmol), 3-ethynylperylene (72 mg, 0.26 mmol), EtMgBr (0.22 mL, 0.22 mmol, 1 M in THF), THF (8 mL); chromatography on silica gel, eluting with ethylacetate–cyclohexane (v/v 15/85) to give 28 mg (29%) of **9** as a dark green solid: mp >350 °C. ^1H NMR (400 MHz, $\text{CDCl}_3\text{--CCl}_4$ (v/v 50/50)): 8.37 (d, 2H, $^4J = 3.6$ Hz), 8.10 (d, 4H, $^3J = 7.2$ Hz), 8.05 (d, 2H, $^3J = 7.2$ Hz), 7.95 (m, 4H), 7.75 (d, 2H, $^3J = 8.4$ Hz), 7.67 (s, 1H), 7.59 (m, 4H), 7.42–7.33 (m, 8H), 7.30 (d, 2H, $^3J = 8.0$ Hz), 7.00 (dd, 2H, $^3J = 8.0$ Hz, $^4J = 2.0$ Hz), 6.87 (d, 2H, $^4J = 3.6$ Hz), 3.87 (s, 6H), 2.77 (q, 4H, $^3J = 7.4$ Hz), 1.14 (t, 6H, $^3J = 7.4$ Hz). ^{13}C NMR (100 MHz, $\text{CDCl}_3\text{--CCl}_4$ (v/v 50/50)): 158.2, 151.1, 143.2, 135.0, 134.8, 133.4, 132.4, 131.6, 131.3, 131.2, 130.8, 130.5, 130.4, 128.8, 128.7, 128.6, 127.8, 127.7, 127.5, 126.6, 124.5, 122.8, 120.4, 120.22, 120.17, 119.8, 119.6, 112.6, 102.8, 97.6, 55.5, 23.7, 15.6. ^{11}B NMR (128 MHz, $\text{CDCl}_3\text{--CCl}_4$ (v/v 50/50)): –6.40 (s). UV–vis (CH_2Cl_2): λ nm (ϵ , $\text{M}^{-1}\text{cm}^{-1}$) 259 (192000), 436 (97000), 465 (120000), 660 (26000), 721 (82500). ES-MS m/z (nature of the peak, relative intensity) 1085.2 ($[\text{M} + \text{H}]^+$, 100). Anal. Calcd for $\text{C}_{73}\text{H}_{49}\text{BN}_2\text{O}_2\text{S}_2$: C, 83.01; H, 4.55; N, 2.58. Found: C, 82.90; H, 4.28; N, 2.43%.

Compound 10. Prepared following experimental conditions 2; from **6a** (50 mg, 0.09 mmol), 9,9-dibutyl-3-ethynyl-9H-fluorene (80 mg, 0.26 mmol), EtMgBr (0.22 mL, 0.22 mmol, 1 M in THF), THF (8 mL); chromatography on silica gel, eluting with ethylacetate–cyclohexane (v/v 4/96) to give 75 mg (76%) of **10** as a green solid: 147 °C (dec). ^1H NMR (400 MHz, $\text{CDCl}_3\text{--CCl}_4$ (v/v 50/50)): 8.34 (d, 2H, $^4J = 4.0$ Hz), 7.69–7.60 (m, 5H), 7.48 (d, 2H, $^3J = 8.0$ Hz), 7.26 (m, 8H), 7.11 (m, 6H), 6.92 (dd, 2H, $^3J = 8.0$ Hz, $^4J = 2.0$ Hz), 3.90 (s, 6H), 3.07 (q, 4H, $^3J = 7.4$ Hz), 1.97–1.84 (m, 8H), 1.49 (t, 6H, $^3J = 7.4$ Hz), 1.10–1.01 (m, 8H), 0.67 (t, 12H, $^3J = 7.4$ Hz), 0.62–0.48 (m, 8H). ^{13}C NMR (100 MHz, $\text{CDCl}_3\text{--CCl}_4$ (v/v 50/50)): 158.0, 150.8, 150.4, 150.1, 142.9, 141.0, 140.1, 133.1, 132.3, 130.9, 130.8, 128.6, 127.5, 127.1, 126.9, 125.5, 124.5, 124.0, 122.7, 120.0, 119.9, 119.1, 113.2, 102.5, 99.3, 55.3, 54.9, 40.5, 26.0, 23.9, 23.3, 16.0, 14.1. ^{11}B NMR (128 MHz, $\text{CDCl}_3\text{--CCl}_4$ (v/v 50/50)): –7.43 (s). UV–vis (CH_2Cl_2): λ nm (ϵ , $\text{M}^{-1}\text{cm}^{-1}$) 298 (110000), 323 (136000), 380 (24000), 650 (30000), 710 (95000). ES-MS m/z (nature of the peak, relative intensity) 1137.2 ($[\text{M} + \text{H}]^+$, 100), 835.2 ($[\text{M} - 9,9\text{-dibutyl-3-ethynyl-9H-fluorene}]^+$, 25). Anal. Calcd for $\text{C}_{77}\text{H}_{77}\text{BN}_2\text{O}_2\text{S}_2$: C, 81.31; H, 6.82; N, 2.46. Found: C, 81.11; H, 6.61; N, 2.16%.

Compound 11. Prepared following general conditions 2; from **6b** (50 mg, 0.09 mmol), 1-ethynylpyrene (60 mg, 0.26 mmol), EtMgBr (0.24 mL, 1 M in THF, 0.24 mmol), THF (8 mL); chromatography (silica gel, cyclohexane/dichloromethane, 60:40) **11** (35 mg, 41%) as a blue solid. ^1H NMR ($\text{CDCl}_3\text{--CCl}_4$ 50/50, 200 MHz): 8.36 (d, 2H, $^3J = 9.2$ Hz), 8.13 (m, 8H), 8.05–7.94 (m, 10H), 7.86–7.78 (m, 5H), 7.03 (dd, 2H, $^3J = 8$ Hz, $^4J = 2$ Hz), 6.86 (m, 2H), 6.69 (m, 4H), 3.76 (s, 6H), 3.19 (s, 6H). ^{13}C NMR ($\text{CDCl}_3\text{--CCl}_4$ 50/50, 75 MHz): 160.1, 157.9, 150.7, 132.5, 132.2, 132.1, 131.51, 131.49, 130.5, 129.6, 128.9, 127.6, 127.5, 127.4, 127.0, 126.6, 126.0, 125.1, 125.0, 124.7, 124.6, 124.2, 120.5,

119.8, 102.1, 97.7, 55.35, 54.6. ^{11}B NMR ($\text{CDCl}_3\text{--CCl}_4$ 50/50, 128 MHz): –6.65 (s). UV–vis (CH_2Cl_2) λ nm (ϵ , $\text{M}^{-1}\text{cm}^{-1}$) = 667 (88500), 618 (27000 sh), 371 (111000), 350 (88500), 286 (175000), 275 (152000), 248 (135000). ES-MS m/z (nature of the peak, relative intensity) 977.3 ($[\text{M} + \text{H}]^+$, 100), 712.3 ($[\text{M} - \text{ethynylpyrene}]^+$, 45). Anal. Calcd for $\text{C}_{69}\text{H}_{43}\text{BN}_2\text{O}_4$: C, 84.83; H, 4.64; N, 2.87. Found: C, 84.67; H, 4.42; N, 2.57%.

Compound 12. Prepared following general procedure 2; from **6b** (46 mg, 0.08 mmol), 4-ethynyltoluene (41 mg, 0.35 mmol), EtMgBr (0.30 mL, 1 M in THF, 0.30 mmol), THF (5 mL); chromatography (silica gel, dichloromethane/cyclohexane, 30:70) gave 50 mg (62%) of **8** as a blue solid: 234 °C (dec). ^1H NMR (DMSO- d_6 , 200 MHz): 8.54 (s, 1H), 8.13–8.05 (m, 6H), 7.24–7.12 (m, 6H), 6.88 (m, 2H), 6.86 (AB_{sys}, 8H, $J_{AB} = 7.9$ Hz, $\nu\delta_{AB} = 52.9$ Hz), 3.81 (s, 6H), 3.77 (s, 6H), 2.23 (s, 6H), ^{13}C NMR (C_6D_6 , 75 MHz): 160.7, 158.5, 150.5, 136.9, 133.2, 132.7, 132.1, 129.3, 128.8, 128.3, 127.6, 127.4, 126.9, 125.9, 123.1, 120.7, 120.2, 114.9, 114.0, 107.1, 102.4, 99.3, 55.0, 54.9, 21.0. ^{11}B NMR (CDCl_3 , 128 MHz): –6.87 (s). UV–vis (CH_2Cl_2) λ nm (ϵ , $\text{M}^{-1}\text{cm}^{-1}$) = 666 (85000), 363 (19000), 268 (99000). ES-MS m/z (nature of the peak, relative intensity) 757.2 ($[\text{M} + \text{H}]^+$, 100). Anal. Calcd for $\text{C}_{51}\text{H}_{41}\text{BN}_2\text{O}_4$: C, 80.95; H, 5.46; N, 3.70. Found: C, 80.72; H, 5.21; N, 3.42%.

Compound 13. Prepared following general procedure 2; from **6c** (100 mg, 0.22 mmol), 1-ethynyltoluene (104 mg, 0.90 mmol), EtMgBr (0.41 mL, 0.41 mmol, 1 M in THF), THF (8 mL); chromatography (silica gel, dichloromethane/cyclohexane, 30:70 to 50:50) gave **8** as a blue, crystalline powder (60 mg, 42%). ^1H NMR (CDCl_3 , 300 MHz): 8.2, (d, 4H, $J = 6.6$ Hz), 7.96 (d, 2H, $J = 6.0$ Hz), 7.92 (s, 1H), 7.61–7.39 (m, 11H), 7.22–7.18 (m, 1H), 6.88 (AB_{sys}, 8H, $J_{AB} = 8.0$, $\nu\delta_{AB} = 24.3$ Hz), 2.27 (s, 6H). ^{13}C NMR (CDCl_3 , 75 MHz): 151.2, 136.8, 133.7, 132.4, 131.3, 130.9, 130.3, 128.3, 128.1, 127.7, 127.6, 124.6, 123.0, 122.4, 121.7, 118.4, 115.8, 98.6, 21.3. ^{11}B NMR (CDCl_3 , 128 MHz): –7.14 (s). UV–vis (CH_2Cl_2) λ nm (ϵ , $\text{M}^{-1}\text{cm}^{-1}$) = 632 (82500), 588 (27000 sh), 269 (12000). ES-MS m/z (nature of the peak, relative intensity) 637.1 ($[\text{M} + \text{H}]^+$, 100). Anal. Calcd for $\text{C}_{47}\text{H}_{33}\text{BN}_2$: C, 88.68; H, 5.23; N, 4.40. Found: C, 88.40; H, 4.95; N, 4.18%.

Compound 14. To a solution of **6a** (50 mg, 0.09 mmol) in THF (6 mL) was added at 25 °C a solution of ethylmagnesium bromide 1 M in THF (0.22 mL, 0.22 mmol). The mixture was stirred for 5 min. The solvent was removed by rotary evaporation. The residue was treated with water and extracted with dichloromethane. The organic extracts were washed with water and then brine and dried over absorbent cotton. The solvent was removed by rotary evaporation. The residue was purified by chromatography on silica gel, eluting with dichloromethane–cyclohexane (v/v 60/40) to give 35 mg (68%) of **14** as a deep blue solid: 257–258 °C. ^1H NMR (200 MHz, $\text{CDCl}_3\text{--CCl}_4$ (v/v 50/50)): 7.84–7.78 (m, 3H), 7.10–7.03 (m, 4H), 6.81 (s, 4H), 3.87 (s, 6H), 2.91 (q, 4H, $^3J = 7.5$ Hz), 1.37 (t, 6H, $^3J = 7.5$ Hz), 0.70 (q, 4H, $^3J = 7.5$ Hz), 0.35 (t, 6H, $^3J = 7.5$ Hz). ^{13}C NMR (100 MHz, $\text{CDCl}_3\text{--CCl}_4$ (v/v 50/50)): 157.8, 150.0, 141.4, 133.9, 130.2, 130.0, 128.5, 127.2, 123.0, 119.2, 119.1, 115.9, 101.5, 96.2, 55.6, 23.5, 15.7, 9.3. ^{11}B NMR (128 MHz, $\text{CDCl}_3\text{--CCl}_4$ (v/v 50/50)): 8.63 (br s). UV–vis (CH_2Cl_2): λ nm (ϵ , $\text{M}^{-1}\text{cm}^{-1}$) 240 (48000), 300 (19000), 360 (13000), 595 (24000), 640 (90000). ES-MS m/z (nature of the peak, relative intensity) 593.2 ($[\text{M} + \text{H}]^+$, 100), 563.1 ($[\text{M} - \text{Et}]^+$, 20). Anal. Calcd for $\text{C}_{35}\text{H}_{37}\text{BN}_2\text{O}_2\text{S}_2$: C, 70.93; H, 6.29; N, 4.73. Found: C, 70.65; H, 6.02; N, 4.55%.

Compound 15. Prepared following experimental conditions 2; from **6a** (50 mg, 0.09 mmol), 4-ethynylpyrene (24 mg, 0.10 mmol), EtMgBr (0.21 mL, 0.21 mmol, 1 M in THF), THF (8 mL); chromatography on silica gel, eluting with dichloromethane–cyclohexane (v/v 30/70) to give 19 mg (28%) of **15** as a green solid: 227 °C (dec). ^1H NMR (400 MHz, $\text{CDCl}_3\text{--CCl}_4$ (v/v 50/50)): 8.47 (1H, $^3J = 8.6$ Hz), 8.12 (m, 2H), 8.02–7.90 (m, 6H), 7.82 (d, 2H, $^4J = 9.6$ Hz), 7.78 (s, 1H), 7.70 (d, 2H, $^4J = 3.2$ Hz), 7.06 (m, 4H), 6.72 (d, 2H, $^3J = 3.2$ Hz), 3.84 (s, 6H), 2.73 (q, 4H, $^3J = 7.4$ Hz), 1.14 (t, 6H, $^3J = 7.4$ Hz), 1.04 (q, 2H, 3J

= 7.8 Hz), 0.34 (t, 3H, $^3J = 7.8$ Hz). ^{13}C NMR (100 MHz, $\text{CDCl}_3\text{-CCl}_4$ (v/v 50/50)): 158.0, 150.6, 142.7, 133.0, 131.9, 131.7, 131.5, 131.4, 130.2, 130.1, 129.6, 128.0, 127.4, 127.3, 126.9, 125.9, 124.9, 124.8, 124.7, 124.6, 124.3, 123.6, 121.1, 119.8, 119.5, 114.4, 102.3, 98.4, 55.5, 23.4, 14.4, 8.9. ^{11}B NMR (128 MHz, $\text{CDCl}_3\text{-CCl}_4$ (v/v 50/50)): 1.07 (s). UV-vis (CH_2Cl_2): λ nm (ϵ , $\text{M}^{-1}\text{cm}^{-1}$) 276 (144000), 286 (148000), 351 (54500), 370 (64000), 681 (71500). ES-MS m/z (nature of the peak, relative intensity) 789.2 ($[\text{M} + \text{H}]^+$, 100). Anal. Calcd for $\text{C}_{51}\text{H}_{41}\text{BN}_2\text{O}_2\text{S}_2$: C, 77.65; H, 5.24; N, 3.55. Found: C, 77.40; H, 5.05; N, 3.38%.

Compound 16. Prepared following experimental conditions 2; from **6c** (100 mg, 0.225 mmol), 1-ethynylpyrene (51 mg, 0.225 mmol), EtMgBr (0.20 mL, 2.2 M in THF, 0.45 mmol), THF (2 mL); chromatography (silica gel, dichloromethane/petroleum ether 30:70), followed by a recrystallization in a dichloromethane/cyclohexane mixture, gave **8** as deep blue crystalline needles (60 mg, 40%). ^1H NMR (CDCl_3 , 400 MHz): 8.36 (d, 1H, $^3J = 9.1$ Hz), 8.19–8.14 (m, 2H), 8.09 (s, 1H), 8.06–7.82 (m, 12H), 7.52–7.37 (m, 2H), 7.29–7.17 (m, 10H), 0.57 (q, 2H, $^3J = 7.2$ Hz), 0.29 (t, 3H, $^3J = 7.3$ Hz). ^{13}C NMR (C_6D_6 , 75 MHz): 151.6, 133.8, 133.1, 132.5, 131.9, 131.9, 130.9, 130.1, 129.1, 128.7, 127.6, 127.1, 127.0, 126.2, 125.5, 125.4, 125.3, 125.2, 124.8, 123.1, 121.2, 118.7, 117.3, 98.0, 27.3, 8.7. ^{11}B NMR (CDCl_3 , 128 MHz): 1.09 (s). FAB^+ m/z : 660.6 ($[\text{M} + \text{H}]^+$, 40), 631.5 ($[\text{M} - \text{Et}, 100]^+$), 435.4 ($[\text{M} - \text{pyr} \equiv, 25]^+$). UV-vis (CH_2Cl_2) λ nm (ϵ , $\text{M}^{-1}\text{cm}^{-1}$) = 614 (78300), 574 (24000 sh), 370 (42000), 351 (37400). ES-MS m/z (nature of the peak, relative intensity) 661.2 ($[\text{M} + \text{H}]^+$, 100), 631.2 ($[\text{M} - \text{ethyl}]^+$, 10). Anal. Calcd for $\text{C}_{49}\text{H}_{33}\text{BN}_2$: C, 89.09; H, 5.04; N, 4.24. Found: C, 88.72; H, 4.75; N, 4.07%.

Preparation of Compound 17. To a solution of 4-iodobenzoylchloride (3.50 g, 13.13 mmol) in anhydrous dichloromethane (100 mL) was added dropwise 2-amino-2-methylpropanol (2.22 g, 24.96 mmol). The solvent was removed by rotary evaporation to afford an amide. Thionyl chloride (15 mL, 0.20 mol) was then slowly added, and the resulting solution was stirred for 30 min at 25 °C. The thionyl chloride was removed in vacuo, and water (250 mL) was added. The solution was made basic with 25% NaOH and extracted with ether. The organic extracts were washed with water and then brine and dried over magnesium sulfate. The solvent was removed by rotary evaporation. The residue was purified by chromatography on alumina, eluting with dichloromethane–cyclohexane (v/v 10/90) to give 3.51 g (88%) of **17** as a white solid: mp 59–60 °C. ^1H NMR (200 MHz, CDCl_3): δ 7.60 (AB, 4H, $^{\text{AB}}J = 8.3$ Hz, $\nu_{\text{AB}} = 16.9$ Hz), 4.00 (s, 2H), 1.28 (s, 6H). ^{13}C NMR (50 MHz, CDCl_3): δ 161.1, 137.2, 129.6, 127.3, 97.9, 79.0, 67.5, 28.2. ES-MS m/z (nature of the peak, relative intensity) 302.1 ($[\text{M} + \text{H}]^+$, 100). Anal. Calcd for $\text{C}_{11}\text{H}_{12}\text{INO}$: C, 43.87; H, 4.02; N, 4.65. Found: C, 43.60; H, 3.74; N, 4.43%.

Preparation of Compound 18. To a solution of **17** (1.50 g, 4.95 mmol) in THF (10 mL) and diisopropylamine (4 mL) were added CuI (59 mg, 0.30 mmol) and $\text{PdCl}_2(\text{PPh}_3)_2$ (208 mg, 0.30 mmol). The solution was argon-degassed for 30 min, and then ethynyltrimethylsilane (736 mg, 7.42 mmol) was added. The solution was stirred for 6 h. The solvent was removed by rotary evaporation. The residue was treated with water and extracted with dichloromethane. The organic extracts were washed with water and then brine and dried over magnesium sulfate. The solvent was removed by rotary evaporation. The residue was purified by chromatography on alumina, eluting with dichloromethane–cyclohexane (v/v 10/90) to give 1.33 g (98%) of **18** as a white solid: mp 92–93 °C. ^1H NMR (200 MHz, CDCl_3): δ 7.63 (AB, 4H, $^{\text{AB}}J = 8.5$ Hz, $\nu_{\text{AB}} = 75.2$ Hz), 4.03 (s, 2H), 1.32 (s, 6H), 0.21 (s, 9H). ^{13}C NMR (50 MHz, CDCl_3): δ 161.4, 131.7, 127.9, 127.8, 125.8, 104.4, 96.5, 79.0, 67.6, 28.3, –0.2. ES-MS m/z (nature of the peak, relative intensity) 272.2 ($[\text{M} + \text{H}]^+$, 100). Anal. Calcd for $\text{C}_{16}\text{H}_{21}\text{NOSi}$: C, 70.80; H, 7.80; N, 5.16. Found: C, 70.69; H, 7.70; N, 5.04%.

Preparation of Compound 19. To a solution of **18** (1.25 g, 4.61 mmol) in THF (20 mL) was added a solution of K_2CO_3 (3.19 g, 23.03 mmol) in water (10 mL) and methyl alcohol (3 mL). The mixture was stirred for 1 h. The solvent was removed by rotary evaporation. The

residue was treated with water and extracted with dichloromethane. The organic extracts were washed with water and then brine and dried over magnesium sulfate. The solvent was removed by rotary evaporation. The residue was purified by chromatography on alumina, eluting with dichloromethane–cyclohexane (v/v 10/90) to give 0.91 g (99%) of **19** as a white solid: mp 77–78 °C. ^1H NMR (200 MHz, CDCl_3): δ 7.70 (AB_{sys}, 4H, $^{\text{AB}}J = 8.6$ Hz, $\nu_{\text{AB}} = 74.7$ Hz), 4.10 (s, 2H), 3.17 (s, 1H), 1.38 (s, 6H). ^{13}C NMR (50 MHz, CDCl_3): δ 161.4, 132.0, 128.2, 128.1, 124.8, 83.1, 79.2, 79.1, 67.7, 28.4. ES-MS m/z (nature of the peak, relative intensity) 200.1 ($[\text{M} + \text{H}]^+$, 100). Anal. Calcd for $\text{C}_{13}\text{H}_{13}\text{NO}$: C, 78.36; H, 6.58; N, 7.03. Found: C, 78.24; H, 6.42; N, 6.92%.

General Procedure Following Experimental Conditions 3 for the Fluoro Substitution by Two Different Alkyne Moieties Leading to Compounds 20a–c. Two Schlenk flasks were, respectively, charged with **19**, THF (6 mL), and 4-ethynylpyrene, THF (6 mL). A solution of ethylmagnesium bromide in THF was then added dropwise in each Schlenk flask, and the mixtures were stirred at 50 °C for 2 h. These mixtures were then added successively at 25 °C via a cannula to a solution of dibenzopyrrometheneboron difluoride in anhydrous THF. The mixture was stirred at 70 °C for 16 h, and the solvent was removed by rotary evaporation. The residue was treated with water and extracted with dichloromethane. The organic extracts were washed with water and dried over absorbent cotton. The solvent was removed by rotary evaporation. The residue was purified by chromatography on silica gel.

Compound 20a. Prepared following experimental conditions 3; from **19** (90 mg, 0.45 mmol), THF (6 mL), 4-ethynylpyrene (102 mg, 0.45 mmol), THF (6 mL), ethylmagnesium bromide (0.42 mL, 0.42 mmol, 1 M in THF), and **6a** (200 mg, 0.35 mmol) in anhydrous THF (15 mL); chromatography on silica gel, eluting with dichloromethane–cyclohexane (v/v 85/15) to dichloromethane–cyclohexane (v/v 80/20) to give 146 mg (43%) of **20a** as a green solid: 162 °C (dec). ^1H NMR (400 MHz, $\text{CDCl}_3\text{-CCl}_4$ (v/v 50/50)): 8.36 (d, 2H, $^4J = 3.8$ Hz), 8.23 (d, 1H, $^3J = 9.0$ Hz), 8.08 (d, 2H, $^3J = 7.5$ Hz), 7.98–7.90 (m, 5H), 7.77 (t, 3H, $^3J = 7.5$ Hz), 7.71 (d, 2H, $^3J = 8.0$ Hz), 7.66 (s, 1H), 7.36 (s, 2H), 7.10–7.04 (m, 4H), 6.94 (d, 2H, $^3J = 3.5$ Hz), 4.05 (s, 2H), 3.89 (s, 6H), 2.87 (q, 4H, $^3J = 7.4$ Hz), 1.36 (s, 6H), 1.27 (t, 6H, $^3J = 7.4$ Hz). ^{13}C NMR (100 MHz, $\text{CDCl}_3\text{-CCl}_4$ (v/v 50/50)): 161.8, 158.2, 151.0, 143.1, 133.4, 132.4, 131.9, 131.5, 131.4, 131.3, 130.5, 129.9, 128.7, 128.4, 127.7, 127.5, 127.4, 127.3, 126.7, 126.3, 125.9, 125.02, 127.97, 124.6, 124.5, 124.1, 120.3, 120.2, 119.8, 112.7, 102.9, 98.7, 97.8, 79.1, 67.7, 55.5, 28.6, 23.7, 15.8. ^{11}B NMR (128 MHz, $\text{CDCl}_3\text{-CCl}_4$ (v/v 50/50)): –7.64 (s). UV-vis (CH_2Cl_2): λ nm (ϵ , $\text{M}^{-1}\text{cm}^{-1}$) 351 (65000), 371 (79000), 650 (20000), 710 (79000). ES-MS m/z (nature of the peak, relative intensity) 958.1 ($[\text{M} + \text{H}]^+$, 100), 732.2 ($[\text{M} - \mathbf{19}]^+$, 20). Anal. Calcd for $\text{C}_{62}\text{H}_{48}\text{BN}_3\text{O}_3\text{S}_2$: C, 77.73; H, 5.05; N, 4.39. Found: C, 77.54; H, 4.73; N, 4.18%.

Compound 20b. Prepared following experimental conditions 3; from **19** (92 mg, 0.46 mmol), THF (3 mL), 1-ethynylpyrene (104 mg, 0.46 mmol), THF (3 mL), ethylmagnesium bromide (0.42 mL, 0.42 mmol, 1 M in THF), and **6b** (200 mg, 0.35 mmol) in anhydrous THF (10 mL); chromatography on silica gel, eluting with petroleum ether–dichloromethane (v/v 50/50) to give 185 mg (56%) of **20b** as blue crystals. ^1H NMR ($\text{CDCl}_3/\text{CCl}_4$ 50/50, 300 MHz): 8.34 (d, 1H, $^3J = 9.0$ Hz), 8.20–8.00 (m, 6H), 7.99–7.94 (m, 5H), 7.85–7.74 (m, 6H), 7.06 (dd, 2H, $^3J = 8.8$ Hz, $^4J = 2.2$ Hz), 6.97–6.1 (d, 8H), 4.09 (s, 2H), 3.79 (s, 6H), 3.62 (s, 6H), 1.39 (s, 6H). ^{13}C NMR+ DEPT ($\text{CDCl}_3/\text{CCl}_4$ 50/50, 75 MHz): 161.9, 160.1, 157.7, 150.1, 132.5, 131.95, 131.9, 131.3, 131.2, 131.1, 130.4, 129.4, 128.8, 128.1, 127.6, 127.5, 127.45, 127.2, 126.5, 126.4, 126.2, 126.0, 125.1, 125.05, 125.0, 124.4, 124.2, 120.3 (CH), 119.9, 119.8, 114.4, 113.5, 102.0, 98.9, 97.1, 79.1, 55.5, 55.2, 28.4. UV-vis (CH_2Cl_2) λ nm (ϵ , $\text{M}^{-1}\text{cm}^{-1}$) = 667 (93000), 368 (73200), 350 (60500), 286 (99000). ES-MS m/z (nature of the peak, relative intensity) 950.2 ($[\text{M} + \text{H}]^+$, 100), 751.2 ($[\text{M} - \mathbf{19}]^+$, 15). Anal. Calcd for $\text{C}_{64}\text{H}_{48}\text{BN}_3\text{O}_5$: C, 80.92; H, 5.09; N, 4.42. Found: C, 80.77; H, 4.81; N, 4.19%.

Compound 20c. Prepared following experimental conditions 3; from **19** (175 mg, 0.88 mmol), THF (6 mL), 4-ethynylpyrene (199 mg, 0.88 mmol), THF (6 mL), ethylmagnesium bromide, (0.81 mL, 0.81 mmol, 1 M in THF), and **6c** (300 mg, 0.675 mmol) in anhydrous THF (15 mL); chromatography on silica gel, eluting with dichloromethane–cyclohexane (gradient v/v 85/15 to 100/00) to give 50 mg (9%) of **20c** as a blue powder. ^1H NMR (400 MHz, CDCl_3): 8.28 (d, 4H, $^4J = 9.0$ Hz), 8.22–8.12 (m, 4H), 8.07 (s, 1H), 8.02–7.92 (m, 7H), 7.81 (d, 2H, $^3J = 7.9$ Hz), 7.69–7.60 (m, 4H), 7.52–7.47 (m, 2H), 7.42–7.37 (m, 4H), 7.32–7.23 (m, 5H), 6.75 (d, 2H, $^3J = 8.7$ Hz), 4.07 (s, 2H), 1.36 (s, 6H). ^{13}C NMR (100 MHz, CDCl_3): 151.9, 134.3, 132.7, 132.4, 131.8, 131.6, 131.5, 131.4, 130.9, 129.9, 129.4, 129.2, 128.8, 128.2, 128.0, 127.9, 127.7, 127.6, 126.7, 126.6, 126.3, 125.5, 125.4, 125.2, 124.8, 124.7, 124.5, 123.6, 120.0, 118.8, 116.2, 104.0, 91.6, 79.5, 28.8. ^{11}B NMR (128 MHz, CDCl_3): –7.16 (s). UV–vis (CH_2Cl_2): λ nm (ϵ , $\text{M}^{-1} \text{cm}^{-1}$) 287 (79900), 350 (48300), 368 (52600), 634 (82900). ES-MS m/z (nature of the peak, relative intensity) 830.2 ($[\text{M} + \text{H}]^+$, 100), 631.2 ($[\text{M} - 18]^+$, 35). Anal. Calcd for $\text{C}_{60}\text{H}_{40}\text{BN}_3\text{O}$: C, 86.85; H, 4.86; N, 5.06. Found: C, 86.58; H, 4.72; N, 4.80%.

General Procedure Following Experimental Conditions 4 for the Hydrolysis of the Oxazoline Leading to Compounds 21a–c. To a solution of the dissymmetric bodipy (**20a–c**) in THF was added H_2SO_4 . The mixture was stirred at 75 °C for 1 h and neutralized at 25 °C with a saturated solution of NaHCO_3 . The solvent was removed by rotary evaporation. The residue was treated with water and extracted with dichloromethane. The organic extracts were washed with water and dried over absorbent cotton. The solvent was removed by rotary evaporation to give the corresponding amino ester. THF (40 mL) and a saturated solution of sodium methoxide in methyl alcohol (6 mL) were then added, and the solution was stirred at 25 °C for 10 min. The mixture was neutralized with a solution of H_2SO_4 3 M, and the solvent was removed by rotary evaporation. The residue was treated with water and extracted with dichloromethane. The organic extracts were washed with water and dried over absorbent cotton. The residue was purified by chromatography on silica gel.

Compound 21a. Prepared following experimental conditions 4; from **20a** (145 mg, 0.15 mmol), THF (40 mL), H_2SO_4 (5 mL, 3 M in water); chromatography on silica gel, eluting with dichloromethane–cyclohexane (v/v 50/50) to dichloromethane to give 112 mg (80%) of **21a** as a green solid: 132 °C (dec). ^1H NMR (400 MHz, $\text{CDCl}_3\text{–CCl}_4$ (v/v 50/50)): 8.39 (d, 2H, $^4J = 3.8$ Hz), 8.30 (d, 1H, $^3J = 9.1$ Hz), 8.06 (m, 2H), 7.96–7.88 (m, 5H), 7.81 (d, 1H, $^4J = 3.9$ Hz), 7.66 (d, 2H, $^3J = 8.7$ Hz), 7.62 (s, 1H), 7.50 (AB_{sys}, 4H, $^{\text{AB}}J = 8.5$ Hz, $\nu\delta_{\text{AB}} = 269.7$ Hz), 7.28 (d, 2H, $^4J = 2.5$ Hz), 6.97 (d, 2H, $^3J = 3.8$ Hz), 6.93 (dd, 2H, $^3J = 4.3$ Hz, $^4J = 1.0$ Hz), 3.88 (s, 3H), 3.87 (s, 6H), 2.90 (q, 4H, $^3J = 7.4$ Hz), 1.29 (t, 6H, $^3J = 7.4$ Hz). ^{13}C NMR (100 MHz, $\text{CDCl}_3\text{–CCl}_4$ (v/v 50/50)): 166.3, 158.2, 150.9, 142.9, 133.3, 132.3, 132.0, 131.5, 131.4, 131.3, 130.6, 130.5, 130.3, 129.8, 129.1, 128.6, 128.4, 127.59, 127.55, 127.51, 127.3, 126.6, 125.9, 125.0, 124.7, 124.6, 124.2, 120.3, 120.2, 119.8, 112.9, 102.6, 98.5, 98.0, 55.3, 51.9, 23.7, 15.8. ^{11}B NMR (128 MHz, $\text{CDCl}_3\text{–CCl}_4$ (v/v 50/50)): –7.00 (s). UV–vis (CH_2Cl_2): λ nm (ϵ , $\text{M}^{-1} \text{cm}^{-1}$) 351 (655000), 371 (79000), 650 (sh, 21000), 717 (83000). ES-MS m/z (nature of the peak, relative intensity) 919.2 ($[\text{M} + \text{H}]^+$, 100), 694.2 ($[\text{M} - \text{ethynylpyrene}]^+$, 25). Anal. Calcd for $\text{C}_{59}\text{H}_{43}\text{BN}_2\text{O}_4\text{S}_2$: C, 77.12; H, 4.72; N, 3.05. Found: C, 77.02; H, 4.69; N, 2.84%.

Compound 21b. Prepared following experimental conditions 4; from **20b** (105 mg, 0.11 mmol), THF (40 mL), H_2SO_4 (5 mL, 3 M in water); chromatography on silica gel eluting with dichloromethane/cyclohexane (v/v 50/50) to give 67 mg (67%) of **21b** as a blue solid. ^1H NMR ($\text{CDCl}_3/\text{CCl}_4$ 50/50, 400 MHz): 8.28 (d, 1H, $^3J = 9.0$ Hz), 8.14–8.00 (m, 6H), 7.99–7.95 (m, 5H), 7.82–7.79 (m, 6H), 7.14 (d, 2H, $^3J = 9.0$ Hz), 6.93–6.90 (m, 8H), 3.89 (s, 3H), 3.81 (s, 6H), 3.59 (s, 6H). ^{13}C NMR (100 MHz, $\text{CDCl}_3\text{–CCl}_4$ (v/v 50/50)): 167.2, 164.1, 153.4, 145.4, 132.3, 131.7, 131.6, 131.5, 130.8, 130.3, 129.8, 129.2, 128.5, 127.9, 127.6, 126.4, 125.5, 125.4, 124.8, 124.7, 124.5, 120.3, 102.6, 97.4, 55.5,

52.4. UV–vis (CH_2Cl_2) λ nm (ϵ , $\text{M}^{-1} \text{cm}^{-1}$) = 669 (70000), 616 (sh, 21000), 368 (55000), 350 (45000). ES-MS m/z (nature of the peak, relative intensity) 911.2 ($[\text{M} + \text{H}]^+$, 100), 751.2 ($[\text{M} - \text{ethynylpyrene}]^+$, 25). Anal. Calcd for $\text{C}_{61}\text{H}_{43}\text{BN}_2\text{O}_6$: C, 80.44; H, 4.76; N, 3.08. Found: C, 80.22; H, 4.49; N, 2.68%.

Compound 21c. Prepared following experimental conditions 4; from **20c** (50 mg, 0.06 mmol), THF (20 mL), H_2SO_4 (2.5 mL, 3 M in water); chromatography on silica gel, eluting with dichloromethane–cyclohexane (v/v 50/50) to dichloromethane to give 41 mg (86%) of **21c** as a blue solid. ^1H NMR (400 MHz, $\text{CDCl}_3\text{–CCl}_4$ (v/v 50/50)): 8.27 (d, 1H, $^3J = 9$ Hz), 8.21 (d, 4H, $^3J = 7.5$ Hz), 8.15–8.13 (m, 2H), 8.07 (s, 1H), 8.03–7.93 (m, 6H), 7.82–7.76 (m, 3H), 8.52 (d, 2H, $^3J = 7.6$ Hz), 7.52–7.48 (m, 2H), 7.39–7.43 (m, 4H), 7.33–7.25 (m, 5H), 6.78 (d, 2H, $^3J = 8.5$ Hz), 3.88 (s, 3H). ^{13}C NMR (100 MHz, $\text{CDCl}_3\text{–CCl}_4$ (v/v 50/50)): 167.2, 151.9, 134.3, 132.7, 132.3, 131.8, 131.6, 131.5, 131.3, 130.9, 130.0, 129.9, 129.4, 129.1, 128.8, 128.6, 128.2, 128.0, 127.9, 127.6, 126.6, 126.3, 125.5, 125.4, 125.2, 124.8, 124.7, 124.5, 123.6, 119.9, 118.8, 116.2, 99.4, 97.6, 91.3, 86.6, 52.4. ^{11}B NMR (128 MHz, $\text{CDCl}_3\text{–CCl}_4$ (v/v 50/50)): –7.01 (s). UV–vis (CH_2Cl_2): λ nm (ϵ , $\text{M}^{-1} \text{cm}^{-1}$) 286 (79900), 350 (50000), 368 (55100), 634 (92300). ES-MS m/z (nature of the peak, relative intensity) 791.2 ($[\text{M} + \text{H}]^+$, 100), 631.2 ($[\text{M} - \text{ethynylpyrene}]^+$, 25). Anal. Calcd for $\text{C}_{57}\text{H}_{35}\text{BN}_2\text{O}_2$: C, 86.58; H, 4.46; N, 3.54. Found: C, 86.39; H, 4.18; N, 3.11%.

Preparation of Compound 22a. Step 1: to a solution of **21a** (39 mg, 0.04 mmol) in THF (15 mL) was added a solution of sodium hydroxide (4 mg, 0.08 mmol) in H_2O (3 mL) and MeOH (10 mL). The mixture was stirred at 25 °C for one night and neutralized with a saturated solution of NH_4Cl . The solvent was removed by rotary evaporation. The residue was treated with water and extracted with dichloromethane. The organic extracts were washed with water and dried over absorbent cotton. The solvent was removed by rotary evaporation to give the corresponding carboxylic acid. Anhydrous CH_2Cl_2 (10 mL), DMAP (10 mg, 0.08 mmol), EDCI (15 mg, 0.08 mmol), and *N*-hydroxysuccinimide (9 mg, 0.08 mmol) were then added, and the solution was stirred for 1 h. The solvent was removed by rotary evaporation. The residue was treated with water and extracted with dichloromethane. The organic extracts were washed with water and dried over absorbent cotton. The residue was purified by chromatography on silica gel, eluting with dichloromethane–cyclohexane (v/v 80/20) to dichloromethane to give 29 mg (67%) of the NHS derivative as a green solid. UV–vis (CH_2Cl_2): λ nm (ϵ , $\text{M}^{-1} \text{cm}^{-1}$) 351 (64000), 371 (79000), 650 (sh, 21000), 718 (82000).

Step 2: a solution of the NHS derivative (20 mg, 0.02 mmol) in *n*-propylamine (4 mL) was stirred at 25 °C for 5 min. The solvent was removed by rotary evaporation. The residue was treated with water and extracted with dichloromethane. The organic extracts were washed with water and dried over absorbent cotton. The residue was purified by chromatography on silica gel, eluting with dichloromethane to give 15 mg (81%) of **22a** as a green solid: 148 °C (dec). ^1H NMR (400 MHz, $\text{CDCl}_3\text{–CCl}_4$ (v/v 50/50)): 8.35 (d, 2H, $^4J = 3.96$ Hz), 8.19 (d, 1H, $^3J = 8.8$ Hz), 8.08 (d, 2H, $^3J = 7.9$ Hz), 7.99–7.89 (m, 6H), 7.81 (d, 2H, $^3J = 8.8$ Hz), 7.75 (d, 1H, $^3J = 8.0$ Hz), 7.68 (s, 1H), 7.53 (d, 2H, 8.9), 7.39 (d, 2H, $^4J = 2.2$ Hz), 7.13–7.09 (m, 4H), 6.93 (d, 2H, $^3J = 3.56$ Hz), 3.91 (s, 6H), 3.38 (q, 2H, $^3J = 7.5$ Hz), 2.85 (q, 4H, $^3J = 7.4$ Hz), 1.62 (m, 2H, $^3J = 7.5$ Hz), 1.24 (t, 6H, $^3J = 7.4$ Hz), 0.99 (t, 3H, $^3J = 7.5$ Hz). ^{11}B NMR (128 MHz, $\text{CDCl}_3\text{–CCl}_4$ (v/v 50/50)): –7.38 (s). ES-MS m/z (nature of the peak, relative intensity) 946.2 ($[\text{M} + \text{H}]^+$, 100), 720.2 ($[\text{M} - \text{ethynylpyrene}]^+$, 25). Anal. Calcd for $\text{C}_{61}\text{H}_{48}\text{BN}_3\text{O}_3\text{S}_2$: C, 77.45; H, 5.11; N, 4.44. Found: C, 77.23; H, 4.92; N, 4.21%.

■ ASSOCIATED CONTENT

Supporting Information. General methods, details of the X-ray crystal structure determination for compounds **6c**, **8**, **11**, and **13–16**, as well as crystal packing, absorption, emission and

excitation spectra for all compounds, analytical data, and NMR plots for all compounds are provided in this section. This material is available free of charge via the Internet at <http://pubs.acs.org>.

AUTHOR INFORMATION

Corresponding Author

*E-mail: gulrich@unistra.fr; ziessel@unistra.fr.

ACKNOWLEDGMENT

The authors thank the CNRS and UdS for partial funding. ANR is thankful for financial support. We also acknowledge the CNRS providing research facilities and financial support and Professor Jack Harrowfield (ISIS, Strasbourg) for commenting on the manuscript before publication.

REFERENCES

- (1) (a) Weissleder, R. *Nat. Biotechnol.* **2001**, *19*, 316–317. (b) Weissleder, R.; Ntziachristos, V. *Nature Med.* **2003**, *9*, 123–128.
- (2) (a) Weissleder, R.; Tung, C.-H.; Mahmood, U.; Bogdanov, A., Jr. *Nat. Biotechnol.* **1999**, *17*, 375–378. (b) Frangioni, J. V. *Curr. Opin. Chem. Biol.* **2003**, *7*, 626–634. (c) Lavis, L. D.; Raines, R. T. *ACS Chem. Biol.* **2008**, *3*, 142–155.
- (3) Gomez-Hens, A.; Aguilar-Caballeros, M. P. *Trends Anal. Chem.* **2004**, *23*, 127–136.
- (4) Haugland, R. P. In *Handbook of Molecular Probes and Research Products*; 9th ed.; Molecular Probes, Inc.: Eugene, OR, 2002.
- (5) (a) Loudet, A.; Burgess, K. *Chem. Rev.* **2007**, *107*, 4891–4932. (b) Ulrich, G.; Harriman, A.; Ziessel, R. *Angew. Chem., Int. Ed.* **2008**, *47*, 1202–1219.
- (6) (a) Dost, Z.; Atilgan, S.; Akkaya, E. U. *Tetrahedron* **2006**, *62*, 8484–8488. (b) Yu, Y.-H.; Descalzo, A. B.; Shen, Z.; Röhr, H.; Liu, Q.; Wang, Y.-W.; Spieles, M.; Li, Y.-Z.; Rurack, K.; You, X.-Z. *Chem. Asian J.* **2006**, *1*–2, 176–187. (c) Atilgan, S.; Ekmekci, Z.; Lale, A.; Dogan, G.; Akkaya, E. U. *Chem. Commun.* **2006**, 4398–4400. (d) Ziessel, R.; Ulrich, G.; Harriman, A.; Alamiry, M. A. H.; Stewart, B.; Retailleau, P. *Chem.—Eur. J.* **2009**, *15*, 1359–1369.
- (7) (a) Ziessel, R.; Bura, T.; Olivier, J.-H. *Synlett* **2010**, 2304–2310. (b) Bura, T.; Retailleau, P.; Ziessel, R. *Angew. Chem., Int. Ed.* **2010**, *49*, 6659–6663.
- (8) (a) Rohand, T.; Qin, W.; Boens, N.; Dehaen, W. *Eur. J. Org. Chem.* **2006**, 4658–4663. (b) Li, L.; Han, J.; Nguyen, B.; Burgess, K. *J. Org. Chem.* **2008**, *73*, 1963–1970. (c) Li, L.; Nguyen, B.; Burgess, K. *Biorg. Med. Chem. Lett.* **2008**, *18*, 3112.
- (9) (a) Rihn, S.; Retailleau, P.; Bugsaliewicz, N.; De Nicola, A.; Ziessel, R. *Tetrahedron Lett.* **2009**, *50*, 7008–7013. (b) Galangau, O.; Dumas-Verdes, C.; Méallet-Renault, R.; Clavier, G. *Org. Biomol. Chem.* **2010**, *8*, 4546–4553.
- (10) (a) Wan, C.-W.; Burghart, A.; Chen, J.; Bergström, F.; Johansson, L. B.-A.; Wolford, M. F.; Kim, T. G.; Topp, M. R.; Hochstrasser, R. M.; Burgess, K. *Chem.—Eur. J.* **2003**, *9*, 4430–4431. (b) Cakmak, Y.; Akkaya, E. U. *Org. Lett.* **2009**, *11*, 85–88. (c) Bonardi, L.; Ulrich, G.; Ziessel, R. *Org. Lett.* **2008**, *10*, 2183–2186. (d) Donur, V. R.; Zhu, S.; Green, S.; Liu, H. *Polymer* **2010**, *51*, 5359–5368.
- (11) (a) Wada, M.; Ito, S.; Uno, H.; Murashima, T.; Ono, N.; Urano, T.; Urano, Y. *Tetrahedron Lett.* **2001**, *42*, 6711–6713. (b) Shen, Z.; Röhr, H.; Rurack, K.; Uno, H.; Spieles, M.; Schulz, B.; Reck, G.; Ono, N. *Chem.—Eur. J.* **2004**, *10*, 4853–4871. (c) Kang, H. C.; Haugland, R. P. US Patent 5433896, 1995. (d) Wu, Y.; Klaubert, D. H.; Kang, H. C.; Zhang, Y.-Z. US Patent 6005113, 1999. (e) Umezawa, K.; Matsui, A.; Nakamura, Y.; Citterio, D.; Suzuki, K. *Chem.—Eur. J.* **2009**, *15*, 1096–1106. (f) Descalzo, A. B.; Xu, H.-J.; Xue, Z.-L.; Hoffmann, K.; Shen, Z.; Weller, M. G.; You, X.-Z.; Rurack, K. *Org. Lett.* **2008**, *10*, 1581–1584. (g) Umezawa, K.; Nakamura, Y.; Makino, H.; Citterio, D.; Suzuki, K. *J. Am. Chem. Soc.* **2008**, *130*, 1550–1551.
- (12) (a) Gorma, A.; Killoran, J.; O'Shea, C.; Kenna, T.; Gallagher, W. M.; O'Shea, D. F. *J. Am. Chem. Soc.* **2004**, *126*, 10619–10631. (b) Hall, M. J.; McDonnell, S. O.; Killoran, J.; O'Shea, D. F. *J. Org. Chem.* **2005**, *70*, 5571–5578. Zhao, W.; Carreira, E. M. *Chem.—Eur. J.* **2006**, *12*, 7254–7263.
- (13) (a) Burghart, A.; Kim, H.; Welch, M. B.; Thorensen, L. H.; Reibenspies, J.; Burgess, K. *J. Org. Chem.* **1999**, *64*, 7813–7819. (b) Yamad, K.; Toyota, T.; Takakura, K.; Ishimura, M.; Sugawara, T. *New J. Chem.* **2001**, *25*, 667–669.
- (14) Yakubovskiy, V. P.; Shandura, M. P.; Kovtun, Y. P. *Eur. J. Org. Chem.* **2009**, 3237–3243.
- (15) (a) Zheng, Q.; Xu, G.; Prasad, P. N. *Chem.—Eur. J.* **2008**, *14*, 5812–5819. (b) Didier, P.; Ulrich, G.; Mély, Y.; Ziessel, R. *Org. Biomol. Chem.* **2009**, *7*, 3639–3642.
- (16) (a) Ju, J.; Ruan, C.; Fuller, C. W.; Glazer, A. N.; Mathies, R. A. *Proc. Natl. Acad. Sci. U.S.A.* **1995**, *92*, 4347–4351. (b) Glazer, A. N.; Mathies, R. A. *Curr. Opin. Biotechnol.* **1997**, *8*, 94–102. (c) Burghart, A.; Thoresen, L. H.; Chen, J.; Burgess, K.; Bergström, F.; Johansson, L. B.-A. *Chem. Commun.* **2000**, 2203–2204.
- (17) Ziessel, R.; Harriman, A. *Chem. Commun.* **2011**, *47*, 611–631.
- (18) Wan, C.-W.; Burghart, A.; Chen, J.; Bergström, F.; Johansson, L. B.-A.; Wolford, M. F.; Kim, T. G.; Topp, M. R.; Hochstrasser, R. M.; Burgess, K. *Chem.—Eur. J.* **2003**, *9*, 4430–4431. Ziessel, R.; Goze, C.; Ulrich, G.; Césario, M.; Retailleau, P.; Harriman, A.; Rostron, J. P. *Chem.—Eur. J.* **2005**, *11*, 7366–7378.
- (19) (a) Ulrich, G.; Goze, C.; Guardigli, M.; Roda, A.; Ziessel, R. *Angew. Chem., Int. Ed.* **2005**, *44*, 3694–398. *Angew. Chem.* **2005**, *117*, 3760–3764. (b) Goze, C.; Ulrich, G.; Ziessel, R. *J. Org. Chem.* **2007**, *72*, 313–322. (c) Goze, C.; Ulrich, G.; Ziessel, R. *Org. Lett.* **2006**, *8*, 4445–4448. (d) Harriman, A.; Izzet, G.; Ziessel, R. *J. Am. Chem. Soc.* **2006**, *128*, 10868–10875.
- (20) Wu, L.; Loudet, A.; Barhoumi, R.; Burghardt, R. C.; Burgess, K. *J. Am. Chem. Soc.* **2009**, *131*, 9156–9157.
- (21) Jose, J.; Ueno, Y.; Castro, J. C.; Li, L.; Burgess, K. *Tetrahedron Lett.* **2009**, *50*, 6442–6445.
- (22) (a) Ulrich, G.; Goeb, S.; De Nicola, A.; Retailleau, P.; Ziessel, R. *Synlett* **2007**, 1517–1520. (b) Goeb, S.; Ziessel, R. *Org. Lett.* **2007**, *9*, 737–740.
- (23) Goze, C.; Ulrich, G.; Mallon, L. J.; Allen, B. D.; Harriman, A.; Ziessel, R. *J. Am. Chem. Soc.* **2006**, *128*, 10231–10239.
- (24) Kang, H. C.; Haugland, R. P. U.S. Patent 5,433,896, Jul. 18, 1995. Wu, Y.; Klaubert, D. H.; Kang, H. C.; Zhang, Y.-Z. U.S. Patent 6,005,113, Dec. 21, 1999.
- (25) Katritzky, A. R.; Harris, P. A.; Kotali, A. *J. Org. Chem.* **1991**, *56*, 5049–5051.
- (26) Maekawa, E.; Suzuki, Y.; Sugiyama, S. *Chem. Ber.* **1968**, *101*, 847–854.
- (27) Ulrich, G.; Goze, C.; Goeb, S.; Retailleau, P. *New J. Chem.* **2006**, *30*, 982–986.
- (28) Soulié, J.; Cadiot, P. *Bull. Chem. Soc. Fr.* **1966**, 3846–3849.
- (29) Qian, B.; Baek, S. W.; Smith, M. R., III. *Polyhedron* **1999**, *18*, 2405–2414.
- (30) C- or E-borondipyrromethenes are, respectively, defined as aryl- or alkyl-substituted at the boron center (C-Bodipy) and ethynyl-substituted at the boron center (E-Bodipy). Classical BF₂ derivatives are F-Bodipys'.
- (31) Hiraoka, S.; Goda, M.; Shionoya, M. *J. Am. Chem. Soc.* **2009**, *131*, 4592–4593.
- (32) Allen, F. H. *Acta Crystallogr.* **2002**, *B58*, 380–388.
- (33) Shen, Z.; Röhr, H.; Rurack, K.; Uno, H.; Spieles, M.; Schulz, B.; Reck, G.; Ono, N. *Chem.—Eur. J.* **2004**, *10*, 4853–4871.
- (34) Ulrich, G.; Ziessel, R. *J. Org. Chem.* **2004**, *69*, 2070–2083.
- (35) Poronik, Y. M.; Yakubovskiy, V. P.; Shandura, M. P.; Vlasenko, Y. G.; Chernega, A. N.; Kovtun, Y. P. *Eur. J. Org. Chem.* **2010**, 2746–2752.
- (36) Karolin, J.; Johansson, L. B.-A.; Strandberg, L.; Ny, T. *J. Am. Chem. Soc.* **1994**, *116*, 7801–7806.
- (37) Harriman, A. H.; Mallon, L. J.; Goeb, S.; Ulrich, G.; Ziessel, R. *Chem.—Eur. J.* **2009**, *15*, 4553–4564.
- (38) Hissler, M.; Harriman, A.; Khatyr, A.; Ziessel, R. *Chem.—Eur. J.* **1999**, *5*, 3366–3378.

- (39) (a) Seneclauze, J. B.; Retailleau, P.; Ziessel, R. *New J. Chem.* **2007**, *31*, 1412–1421. (b) Bura, T.; Ziessel, R. *Tetrahedron Lett.* **2010**, *51*, 2875–2879.
- (40) Harriman, A. H.; Izzet, G.; Ziessel, R. *J. Am. Chem. Soc.* **2006**, *128*, 10868–10875.
- (41) Englman, R.; Jortner, J. *Mol. Phys.* **1970**, *18*, 145–164.
- (42) Olmsted, J., III. *J. Phys. Chem.* **1979**, *83*, 2581–2584.
- (43) (a) Niu, S. L.; Ulrich, G.; Ziessel, R.; Kiss, A.; Renard, P.-Y.; Romieu, A. *Org. Lett.* **2009**, *11*, 2049–2052. (b) Niu, S.-L.; Ulrich, G.; Retailleau, P.; Harrowfield, J.; Ziessel, R. *Tetrahedron Lett.* **2009**, *50*, 3840–3844.